AN ABSTRACT OF THE THESIS OF

Mark S. Lorang for the degree of Doctor of Philosophy in

Oceanography presented on April 4, 1997

Title: **Wave Competence and Morphodynamics of Boulder and Gravel Beaches**

Redacted for privacy

Abstract Approved:

Peter C. Klingeman

A reformatted Shields relation, $\tau_{crit} = 0.045(\rho_s - \rho_w)gD_{50}^{0.6}D_{\max}^{0.4}$, is used to estimate the shear stress required to remobilize the maximum-size particles from high-gradient river reaches having bed material ranging in size from gravel to boulders. The analysis uses a mobility ratio, expressed as the fluid shear stress during bank-full conditions, $\tau_b = 1/8\, f_r \rho_w U^2$, over the reformatted Shields entrainment stress calculated from the size of the bed material. The mobility ratio, τ_b / τ_{crit}, for bank-full discharge is much less than unity for most of the 33 sites analyzed. It is concluded that extension of the reformatted Shields equation to flood deposits and boulder-bed rivers to estimate past hydraulic conditions or to determine flushing flows for regulated rivers could result in significant error.

The concept of wave competence is developed here and applied to boulders and gravel on a beach. Two equations are derived, one to estimate critical threshold mass, M_{Ru}, where

$$M_{R_u} = \frac{\rho_s f_{BF} U_{\max} R_u^{\,3} 2\mathrm{f}}{K_r \left(\frac{\rho_s - \rho_w}{\rho_w} \right) g \tan\theta} \qquad \text{(III-41)}$$

and another to estimate minimum stable mass, M_{Hsb}, where

$$M_{H_{sb}} = \frac{\rho_s f_{BF} U_{max} R_u H_{sb}^2 2f}{K_r \left(\frac{\rho_s - \rho_w}{\rho_w} \right) g \tan\theta} \qquad \text{(III-42)}$$

Estimates from III-41 accurately match field data giving the largest boulder transported on a beach during storm events. Equation III-42 predicts stable stone mass in the range defined by the Hudson formula, but has the advantage over the Hudson formula of incorporating the physically important parameters of wave period and swash velocity into a practical expression and thus avoids the need to guess a value for an empirical stability coefficient.

The beach crest is a common morphological feature formed by the deposition of sediment carried up-slope by wave swash. Two equations are derived that relate the height of the beach crest, h_c, to the wave forces and the beach material:

$$h_c = \frac{1}{2} \left(\frac{\rho_s - \rho_w}{\rho_w} \right) \left(\frac{gTD_i \tan\theta}{C_d U_{max}} \right) \qquad \text{(IV-11)}$$

and

$$h_c = \frac{\rho_w H_{sb}^2}{8m} \qquad \text{(IV-15)}$$

Equation IV-11 compares the wave force acting to move a stone up the beach face with a weight force acting to hold the stone in place. Equation IV-15 relates the potential energy per unit area of the beach crest to the total wave energy that lifts and deposits the material above a given sea-level datum. The actual crest height of a natural gravel beach was accurately estimated by both equations.

Wave Competence and Morphodynamics of Boulder and Gravel Beaches

by

Mark S. Lorang

A THESIS

submitted to

Oregon State University

in partial fulfillment of
the requirements for
the degree of

Doctor of Philosophy

Presented April 4, 1997
Commencement June 1997

Doctor of Philosophy thesis of Mark S. Lorang presented on April 4, 1997

APPROVED:

Redacted for privacy

Major Professor representing Oceanography in charge of major

Redacted for privacy

Dean of College of Oceanographic and Atmospheric Sciences

Redacted for privacy

Dean of Graduate School

I understand that my thesis will become part of the permanent collection of Oregon State University libraries. My signature below authorizes release of my thesis to any reader upon request.

Redacted for privacy

Mark S. Lorang, Author

ACKNOWLEDGMENTS

As a young boy, spending countless hours on the gravel beaches of Flathead Lake perfecting the art of skipping rocks, a seed of interest was planted concerning waves and beach processes. It wasn't until later in college that I read a book "Beach Processes and Sedimentation" that I discovered it was possible to spend a life time researching and writing about such subjects. I thank Paul Komar for writing that book and his help in starting my graduate career. More importantly, I thank my father for teaching me a love and appreciation for fly fishing. It was time spent fishing, throughout my graduate studies, that allowed me to leave the science behind and keep a tight line on what is really important in life. So, I would like to thank all my fishing buddies: Ebony, Tom Lippmann, David Egger, Kevin Tillotson, Peter Howd, Peder Allison, Mike Lippmann, Todd Holland and my son, Ian McKenzie and my Dad, for the most recent float in Alice during the final days of finishing this thesis.

Graduate school is a lot like sailing, in that if you are going to sail a boat you have to expect to endure a storm. I was able to survive the worst weather anyone could imagine because I wasn't on a solo voyage. I would like to give my deepest thanks to: Lynne Fessenden, Joe Ortiz, Donna Witter, Jim Tait, Bob Jarrett and Jack Stanford for helping me weather the storm and get my ship back on course. Without their help I would have surely been lost at sea. I would also like to thank my long time friend Jon Jourdonnais for his unconditional support over the years. Larry Small provided me with a student fellowship that made it possible to continue. Many thanks go to Professor Klingeman for serving as my major advisor. He spent a great deal of time reading, editing and helping me to better understand fluvial processes, as well as how to apply those concepts to gravel beaches. Rob Hollman, Bob Duncan, Gordon Grant and Douglas Markle also served on my committee, and I thank them for their support and guidance.

Given all of the scientists I have had the privilege to work with, Bob Jarrett and Jack Stanford remain as the two I most admire. They both guide their research along paths that are of direct significance to the society and environment we live in. I thank them both for their continued and long term support and hope that I can follow their lead.

All it takes is a stroll through the library to realize that everyone, including their dog, has published something and as the years pass the stories will continue to pile up. As I think back on the people I've met pursuing a graduate degree, I realize the common thread that holds us all together is not the science, but our families and friends. Perhaps the worst part about graduate school is that you make close friendships and then everyone moves on. But life continues and the friendships remain. On behalf of Vicki and myself, thanks to: Lynne and Peder, Tom and Diane, Peter and Kathryn, Nathaniel and Sheila, Kevin and Suavie, Dave and Dave (he's a big guy), and June. Thank you Boz for your constant interest and enthusiasm during my return trips to the homeland. Greg, thanks for all the powder shoots and trees we've skied and dicing up the extreme terrain before anyone knew that you could. Fishing with Dave will one day be a book. Thank you Dave for giving me just one more cast, even though we both knew I was stalling for more. Kevin my friend, thanks for all the great beer you've brewed, float trips we've taken, golf and hoop lessons you've endured, trips to Montana, pheasant hunts to cock-bird corner, surveying everything in sight and listening. Tom, what can I say? The rows of cherry trees are pretty straight. Thanks for all the beers, stories, fishing trips, bear chasing adventures and your knack for squeezing in a little time for a friend. Ian and Maddie couldn't be luckier than having you for a godfather. We look forward to lifetime of good times because I know who to call. Diane, thanks for the midnight excitement about drag and coefficients of related nonsense. I missed your sincere honest spirit during these final days. Peter, thanks for looking over my work and providing support in the early years when I was just learning to add, moverover, thanks for calming me down (at 4 am) the night before my prelim. The fishing has been fun and Hosmer will always be hard to top.

Kathryn, good food, good wine and a little banter, thanks for your constant stream of support. Nathaniel, rest assured I will take every opportunity to leave you on the beach with paper, pencil and time to think about perhaps a better way. The enthusiasm and constant support from both you and Sheila were greatly appreciated. Anyone who gets excited about scrubbing a deck on a January morning before they sail has forever earned my admiration and respect. The one person who truly garners all my respect and admiration is Lynne Fessenden. As with Tom, my children are extremely lucky to have Lynne as their godmother to guide them by the simple grace with which she approaches all of life. I just want to be like you Lynne. Thank you all for the good times we've had and those that are soon to come.

The tools for success came from the enduring love of my father and mother. They taught me to look back at the times when there were only a single set of foot prints in the sand and realize they were not always mine. Every step of the way I've had a constant source of encouragement that has come from my friends, my parents and my life partner. I would not have had the strength to finish had it not been for the support of my wife. Vicki, thank you for your love and understanding. Together we have completed this voyage and now, together with Ian and Madeline, we can chart out a new one. Ain't Life Grand!

TABLE OF CONTENTS

TABLE OF CONTENTS (Continued)

TABLE OF CONTENTS (Continued)

CHAPTER 1

WAVE COMPETENCE AND MORPHODYNAMICS OF BOULDER AND GRAVEL BEACHES

GENERAL INTRODUCTION

The general theme of this dissertation is extension of the concept that the size of the largest stone composing a coarse grained deposit reflects the magnitude of the hydraulic event that last transported it. This concept has been referred to in past riverine work as flow competence. It is based on the intuitive notion that threshold shear stress can be inferred from the size of the largest particles transported by open channel flow. This idea is applied here to the beach environment. To do this, the quantitative techniques employed in the riverine environment are modified to apply to wave action on boulder and gravel beaches. Therefore, the term wave competence is used here to refer to the ability of waves to entrain boulder and gravel-size particles composing a beach in a manner similar to the concept of flow competence in rivers.

Three main objectives were addressed. The first objective was to critically examine accepted flow competence techniques as a method for assessing the mobility potential of bank-full discharge events for steep-gradient gravel- and boulder-bed rivers. The question of interest for this first objective was: how useful are the accepted flow competence techniques as a method for predicting the magnitude of discharge required to re-mobilize riverine gravel to boulder size material? Simulating natural flood events is of particular interest as an operational mechanism for enhancing ecological health of regulated rivers (Stanford et al., 1996). The success of flood simulation, aimed at re-mobilizing river bed substratum, is dependent on the accurate estimation of flow-competent conditions from the size of the bed material.

The second objective was to derive two equations for boulders on a beach: one to estimate critical threshold mass and another to estimate minimum stable mass. Both equations include the same physical parameters: stone density, beach slope, breaking wave height, water depth, wave period, run-up height, maximum swash velocity and average swash velocity. These wave-competence equations are useful in the initial evaluation and design of both stable and dynamic shore protection structures constructed with quarry stone. These equations have advantages over traditional shore protection design techniques in that the physically important parameters of wave period and swash velocity are incorporated into simple, yet practical, expressions of wave competence without having to guess at proper values for empirical coefficients.

The third objective was to derive two more equations that relate the height of a gravel beach crest to the wave forces and the beach material. The beach crest is a common morphological feature formed by the deposition of sediment carried up-slope by wave swash. The elevation to which waves can pile gravel is a function of: size and density of the material versus the hydraulic components of swash velocity, wave frequency and run-up height. The first derivation begins with a balance between the wave force acting to move a stone up the beach face and a weight force acting to hold the stone in place. The second derivation relates the potential energy per unit area of the beach crest to the total wave energy that lifted and deposited the material above a given sea-level datum. Both equations rely on the assumption that the wave-competence level is much greater than the threshold entrainment condition for gravel. When this condition is met, then wave swash can pile gravel into a beach crest. Both of these equations could be useful in the design of dynamic shore protection structures composed of gravel-size material.

CHAPTER 2

FLOW COMPETENCE EVALUATION OF FLOODS

ABSTRACT

The concept of flow competence infers threshold shear stress of a flowing fluid from the size of the largest particles transported. The technique includes empirical relations where critical threshold shear stress, τ_{crit}, is represented as a power function of particle diameter, D, in the general form, $\tau_{crit} = aD^b$. A large range of values for the a and b coefficients has been published, with the difference attributed to selective entrainment from a mixed bed of various particle sizes (Komar, 1987a, 1989). The Shields entrainment relation has been re-written (Komar, 1987a) into a flow competence equation, $\tau_{crit} = \theta_{crit}(\rho_s - \rho_w)gD_{50}^{0.6}D_{\max}^{0.4}$, dependent on both the mean and maximum particle diameters and assuming a constant value for the Shields entrainment function, θ_{crit}. This reformatted Shields relation is used here to estimate the shear stress required to remobilize the largest size particles from 33 high-gradient river reaches that have bed material ranging in size from gravel to boulders. The analysis uses a mobility ratio, τ_b/τ_{crit}, expressed as the shear stress, $\tau_b = 1/8 f_r \rho_w U^2$, during bank-full conditions over the reformatted Shields entrainment stress, t_{crit}, calculated from the size of the surface bed material composing each site. The analysis indicates that a bank-full discharge would not mobilize the largest size material for 28 of the 33 sites. Most sites would require a two-fold increase in shear stress to mobilize the river-bed gravel and cobbles present and nearly an order of magnitude increase to entrain boulder size substratum. However, increasing discharge would for the most part only cause over-bank flooding and not result in a corresponding increase in flow depth and shear stress in the river channel. Given that the mobility ratio, τ_b/τ_{crit}, for bank-full discharge is much less than unity, it is concluded that the reformatted Shields relation does not fully represent the sediment transport processes active during floods. Therefore, extension of the reformatted Shields equation to flood

deposits and boulder-bed rivers in order to estimate past hydraulic conditions or to determine flushing flows for regulated rivers could result in significant error.

INTRODUCTION

Gilbert and Murphy (1914) first introduced the concept of flow competence. It is based on the idea that the size of the material a flow can barely move represents a measure of maximum shear stress. Over the last six decades such threshold entrainment has been evaluated by developing empirical curves relating shear stress to the size of largest particles set in motion. This approach to flow competence has been used by fluvial geomorphologists and engineers in attempts to reconstruct the hydraulic conditions of past floods or determine river bed and irrigation channel stability (Hjulstrom 1935; Shields, 1936; Hjulstrom, 1939; White, 1940; Lane and Carlson, 1953, Kellerhals, 1967; Ridder, !967; Scott and Gravlee, 1968; Baker and Ritter, 1973; Bradley and Mears, 1980; Costa, 1983; Andrews, 1983; and 1984; Costa, 1987; Komar, 1987a&b; 1988 and 1989; Komar and Carling, 1991; O'Conner, 1993). One conclusion from this body of work is that using only the size of the largest particle transported to estimate flood hydraulics ignores important physical aspects of threshold entrainment and may lead to significant error.

Threshold entrainment of unconsolidated material by fluid flow is also of interest to river ecologists. Changes in shear stress result in differential transport and deposition of sediment that subsequently induces a related ecosystem response (Lisle, 1989; Von Guerard, P.B., 1989; Shields and Milhous, 1992; Stanford et al., 1996;). Simulating natural floods is of particular interest as an operational mechanism for enhancing ecological health of regulated rivers (Stanford et al., 1996). The success of flood simulation, aimed in part at remobilizing the surface particles composing the river bed, is dependent on the accurate estimation of flow-competence conditions from the size of the bed material. Many factors affect threshold entrainment and related flow-competence equations.

Factors Affecting Threshold Entrainment

The primary factors controlling threshold entrainment are the flow velocity, the particle surface area exposed to the flow and the pivoting angle between particles (Komar and Li, 1986; Li and Komar, 1986; Komar, 1987 a&b; 1989; Kirchner et al., 1990; Bridge, 1992; Carling et al., 1992). The primary forces involved in threshold entrainment are the immersed weight acting to hold a particle to the bed versus the fluid drag and lift forces acting to entrain the particle. Threshold entrainment is achieved when the lift and/or drag forces are able to exceed the effects of the weight force. The drag force is more important than the lift force when a particle is much larger than the underlying bed material. However, the lift force may become more important for threshold entrainment of a small particle sheltered by larger ones. Particle shape, size and factors of packing such as imbrication affect the geometry controlling the effective pivoting angle and the particle surface area exposed to the flow. Therefore, a bed composed of a mixture of sizes and shapes naturally leads to the situation where the critical shear stress necessary for threshold entrainment for any particular size is different than for the situation of uniform particle size (Parker and Klingeman, 1982; Parker et al., 1982; Andrews, 1984; Komar and Li, 1986; Li and Komar, 1986; Hassan and Reid, 1990; Kirchner et al., 1990; Bridge, 1992; Carling et al., 1992).

Turbulence in the flow field is also a factor in threshold entrainment. It affects accurate measures of mean flow velocity, and hence, estimates of mean shear stress acting on the particles that compose the bed. More significantly, the initiation of particle motion involves instantaneous flow velocities and shear stresses rather than mean values of those fluctuating parameters (Kirchner et al., 1990; Whiting and Dietrich, 1990; Komar and Shih, 1992). Hammond et al. (1984), studying gravel threshold in tidal channels, observed that initial gravel motion occurred due to turbulent bursts near the bed at mean flow velocities below theoretical threshold criteria. Drake et al. (1988), working in a mountain stream, observed particle velocities in excess of mean flow velocity that they attributed to

turbulent sweeps (i.e., eddies on the scale of the channel dimensions sweeping across the bed). Obviously, turbulence in the flow field is a very important hydraulic parameter in terms of predicting sediment threshold entrainment.

Grass (1970) hypothesized that threshold entrainment results from the interaction between two statistically random variables: that associated with the fluctuating flow turbulence close to the bed and a second produced by the susceptibility of the particles to movement. When the mean flow velocity increases, the distribution of instantaneous flow stresses produced by the turbulence approaches and finally overlaps the distribution of potential particle susceptibility. Shih and Komar (1990 a&b), utilizing data from Milhous (1973), show that the bedload distribution changes with increasing flow strength. As velocity increases the distribution of the bed load shifts from a Gaussian to a coarse-dominated Rosin distribution similar to that of the bed (Shih and Komar 1990 a&b). Reid and Frostick (1986) examined the frequency distribution of transport efficiency of three rivers and found that distinct modes of efficiency characterized the sediment transport capability of each river. They concluded that the distinct efficiency modes are a product of the particle size distribution of the available bed material and that modal peaks in transport efficiency correspond to modal peaks in the particle size distribution.

Particle Collisions

Another factor not accounted for in the development of flow competence equations is momentum transfer between entrained particles and those held to the bed. Not all entrained particles need come initially from shear stress acting on a stable bed. Cobbles and boulders may be introduced from an eroding bank or localized flow directed into the bed due to either turbulence or flow over obstructions. Turbulence associated with flow in higher-gradient channels can direct flow into the bed and locally scour the channel, resulting in the entrainment of particles not associated with the shear stress due to

mean flow. Therefore, localized scour could introduce entrained particles to a non-competent mean flow. Furthermore, natural beds are never homogeneous throughout, resulting in areas where the substratum could be characterized as an open framework. Such situations would likely result in larger particles resting on smaller ones, effectively lowering their threshold entertainment stress below that predicted for uniform grains and hence resulting in particles being entrained into a mean flow below their theoretical critical threshold conditions.

Each of these factors may add entrained particles to a mean flow below theoretical threshold entrainment levels. Once a particle is entrained it takes very little momentum from the flow to maintain transport. The transport of entrained particles results in collisions with the bed at locations further downstream. Clearly, momentum exchange due to collisions between entrained particles and the bed would increase the ability of a flow to transport an even larger particle. This may be most important in steep gradient cobble and boulder bed rivers and as a bed scouring mechanism during floods. The net result is that paleo-flow estimates based solely only particle size from flood deposits may be significantly in error. Likewise, requested flows from dams aimed at re-mobilizing gravel-cobble sized deposits, based on flow competence techniques derived from those gravel and cobble bars, may be greater than necessary.

The concept of threshold entrainment is rather simple. However, quantifying the many factors and forces that control threshold entrainment is quite difficult. Therefore, an understanding of the possible limiting factors is imperative to proper interpretation of the results that arise through application of flow competence equations that can predict threshold shear stress from the size of the particles composing a river-bed or a flood deposit.

THE DEVELOPMENT OF FLOW COMPETENCE EQUATIONS

Flow Resistance and Shear Stress

Unidirectional turbulent flow in river channels provides a starting point for developing flow competence equations for a mobile bed and for establishing relations for the threshold of particle motion. Extensive discussions may be found in Chow (1959), Henderson (1966), Allen (1970), Vanoni (1975), and other treatises on sediment transport in rivers. Important to sediment entrainment is the frictional drag between the unconsolidated particles composing the river bed and the overlying flow of water. This frictional drag results in a shear stress which is a fluid force applied to the bed. Open channel friction equations provide the starting point for expressing shear stress.

Open channel friction equations include variables representing channel geometry, boundary resistance, and ease of water movement. The Chezy equation is widely used:

$$U = C\sqrt{RS} \qquad \text{(II-1)}$$

where U is the mean velocity C is the Chezy coefficient of flow resistance over the channel, S is the channel slope and R is the hydraulic radius given as A/P where A is channel area and P is the wetted perimeter. Another widely used friction equation is the Darcy-Weisbach equation

$$U = \sqrt{\frac{8}{f_r} gRS} \qquad \text{(II-2)}$$

where f_r is the Darcy-Weisbach friction coefficient and g is the acceleration due to gravity. The Chezy, C, can be equated to the Darcy-Weisbach, f_r, through substitution of II-1 into II-2 for $\sqrt{RS}$, yielding

$$C = \sqrt{\frac{8}{f_r} g} \quad \text{or} \quad f_r = \frac{8g}{C^2}. \qquad \text{(II-3)}$$

The boundary shear stress, τ, at a river bed is a force determined from a force balance on a fluid element in steady uniform flow (Chow,1959; Henderson, 1966; Allen, 1970; Vanoni, 1975). Hydrostatic forces cancel out and the weight component, γALS, over some length, L, in the downstream direction is counter balanced by boundary resistance, τLP

$$\gamma ALS - \tau LP = 0 \tag{II-4}$$

where γ is the specific weight of the fluid. Solving for τ yields

$$\tau = \gamma RS \tag{II-5}$$

Equations II-1 and II-5 may be rearranged in terms of RS

$$RS = \frac{U^2}{C^2} = \frac{\tau}{\gamma} \tag{II-7}$$

and

$$\tau = \gamma \frac{U^2}{C^2} = \left(\frac{g}{C^2}\right)\rho_w U^2. \tag{II-7}$$

Substitution of II-3 for C^2 into II-7 yields

$$\tau = \frac{1}{8} f_r \rho_w U^2 \tag{II-8}$$

where ρ_w is the fluid density. These equations II-5 and II-8 relate shear stress, τ, to water density, channel slope, depth or flow velocity and some estimate of frictional resistance.

Shear stress between a flowing fluid and its potentially mobile bed is the first quantity of interest when evaluating threshold entrainment.

Threshold Entrainment and Flow Competence

Threshold entrainment occurs when the shear force applied to the exposed surface area of a particle exceeds the particle's immersed weight. The size of the largest particle entrained is then a measure of the competence level of the mean flow to transport sediment. This concept of flow competence can be used to express shear stress as a function of particle diameter, D, of a sphere. It is derived from a force balance relation between the immersed weight force and the fluid drag force (Fig. II-1). The immersed weight force, F_{iwt}, is the weight force in air minus the buoyant force when fully submerged and is given as

$$F_{iwt} = (\rho_s - \rho_w) g(\alpha_1 * D^3) \qquad \text{(II-9)}$$

where ρ_s is the density of the particle being entrained and α_1 is shape factor that relates to the particle volume (e.g. $\pi/6$ for a sphere). The fluid drag force, F_d, can be written in the following manner

$$F_d = \tau * D^2 \left(\frac{\alpha_2}{C_p} \right) \qquad \text{(II-10)}$$

where C_p is a packing coefficient and α_2 is a shape factor (e.g. $\pi/4$ for a circle). The ratio α_2/C_p describes the projection surface area exposed to the flow dependent on the size, shape and packing arrangements of particles composing the river bed.

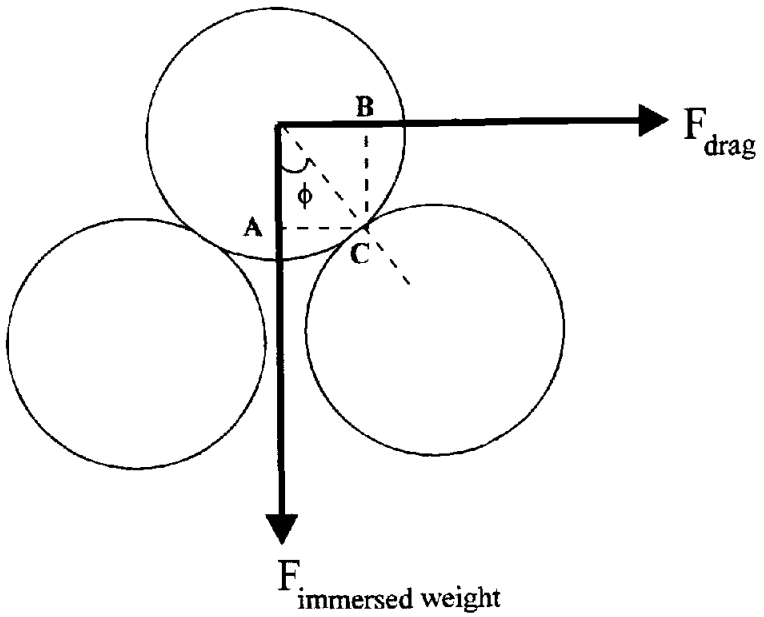

Figure II-1. Schematic depicting the relationship between a drag force associated with a flowing fluid and a weight force acting on a sphere. The angle ϕ reflects the pivoting angle between spheres about the contact point C and is affected by channel slope.

Critical threshold entrainment occurs when the moment of the drag force, F_d, about the pivot point C (Fig. II-1) equals the moment of the immersed weight force, F_{iwt}

$$F_{iwt} * \overline{AC} = F_d * \overline{BC} \tag{II-11}$$

where

$$\overline{AC} = \left(\frac{D}{2}\sin\phi\right) \text{ and } \overline{BC} = \left(\frac{D}{2}\cos\phi\right). \tag{II-12}$$

Substitution of II-12 into II-11 and solving for the coefficients yields

$$C_p \frac{\alpha_1}{\alpha_2}\tan\phi = \frac{\tau_{crit}}{(\rho_s - \rho_w)gD} \tag{II-13}$$

and

$$C_p \frac{\alpha_1}{\alpha_2} \tan\phi = \theta_{crit} \qquad \text{(II-14)}$$

where t_{crit} is the critical shear stress at which threshold entrainment occurs and θ_{crit} is a complex non-dimensional variable dependent on the distributions of particle size, shape and the packing of the bed. Substitution of II-14 into II-13 yields a dimensionless form of the critical shear stress termed the Shields entrainment function

$$\theta_{crit} = \frac{\tau_{crit}}{(p_s - \rho_w)gD}. \qquad \text{(II-15)}$$

Quartz-density spheres in water obey equation II-15 only for $D \geq 6cm$, where θ_{crit} attains a constant value of 0.06 (Bagnold, 1966; Allen, 1970). Solving equation II-15 for the critical shear stress, τ_{crit}, yields a simple flow competence equation

$$\tau_{crit} = 0.06(\rho_s - \rho_w)gD. \qquad \text{(II-16)}$$

applicable to quartz-density spheres for $D \geq 6cm$.

Empirical Flow Competence Equations

Numerous studies have examined relations between flow velocity or shear stress and threshold entrainment that resulted in empirical flow competence equations (Hjulstrom, 1935 and 1939; White 1940; Lane and Carlson, 1953; Wolman and Eiler, 1958; Kellerhals, 1967; Helley, 1969; Baker and Ritter, 1973; Parker et al., 1982; Andrews, 1983; Costa, 1983; Williams, 1983; Andrews, 1984, Komar, 1987 a&b, 1989, O'Conner, 1991). Typically the flow competence equations are in the form of a simple regression between particle diameter and shear stress in the following power relation

$$\tau = aD^b \qquad \text{(II-17)}$$

where b is the slope of the regression line and a is the y-intercept for a log-log plot of stress versus intermediate particle diameter. Komar (1987a) obtained values of 26.6 and

1.21, respectively, for the a and b coefficients utilizing data from floods in boulder bed rivers reported by Costa (1983). Carling (1983) found values of 110 and 0.38 working in low gradient (< 0.002) gravel-bed streams in England. Hammond et al., (1984) found values of 55 and 0.42 with data collected from a tidal channel. These empirical relations are plotted in Figure II-2.

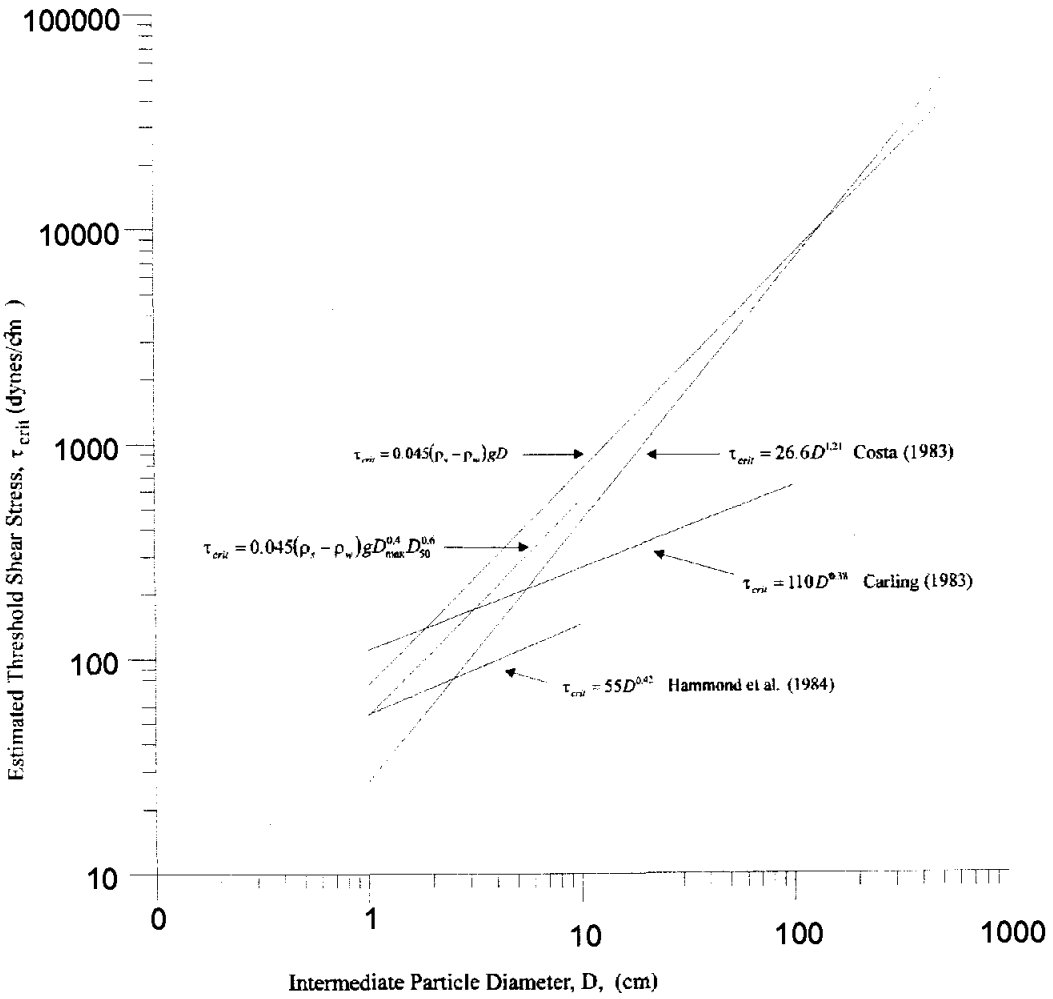

Figure II-2. Comparison of empirical flow competence equations of Costa (1983), Carling (1983) and Hammond et al. (1984) with the Shields and the adjusted Shields flow competence equations II-16 (using $\theta_{crit} = 0.045$ not 0.06) and II-19. The particle diameter D_{max} used in equation II-19 was calculated using a constant ratio of $D_{max}/D = 5$. Stress, τ_{crit}, is given in units of dynes/cm^2 to maintain consistency with published data. The lengths of the regression lines indicate the range of particle diameters for each data set.

The proportionality coefficient a reflects the difference in the overall substratum coarseness between each site. The b coefficient represents the slope of the regression line that ultimately reflects the degree of selective sorting characteristic of each site (Komar, 1987 a&b; 1989; Shih and Komar, 1990; Komar and Carling, 1991; Komar and Shih, 1992). A lower b coefficient or regression line slope reflects a greater degree of sorting by size for a given variation in shear stress (Fig. II-2). This results from particle size distributions specific to individual reaches that respond uniquely to a given distribution of flow stress (Inman, 1949; Carling, 1983; Komar and Li, 1986; Li and Komar, 1986; Komar, 1987 a&b, 1988; Ashworth and Ferguson, 1989; Komar, 1989; Kirchner et al., 1990; Komar and Carling, 1991; Bridge and Bennett, 1992; Komar and Shih, 1992).

The differences in these regression lines also involve uncertainties in using different data sets. These data sets may not have homogeneous data measurement errors, and therefore, do not incorporate the same independent explanatory variables. Flow competence regression equations that result from estimates of flood hydraulics and measured flood deposits would be expected to differ from regression equations that are determined under low flow conditions with careful measurement of hydraulics and initial particle entrainment.

Komar (1986, 1987 see Fig. 3 in each) demonstrates, using data from several locations having naturally differing size, shape and packing conditions of the particles composing the river bed, that regression lines of individual data cross the theoretical threshold curve, equation II-16, at different locations and slopes. Komar (1988) further demonstrates that the measurements can be made to converge if normalized to their respective mean diameters, D_{50} with the following relationship

$$\theta_{crit} = a\left(Di/D_{50}\right)^{b} \qquad \text{(II-18)}$$

where D_i refers to the intermediate diameter of the individual grain to be entrained. The argument presented by Komar (1988) is that this ratio reduces the variance in measured critical threshold stress, produced by the actual pivoting relations that exist in mixed beds, from uniform bed theory, equation II-16. The data reviews of both Miller et al. (1977) and Yalin and Karahan (1979) found that the dimensionless Shields entrainment function, θ_{crit}, approaches a constant value of 0.045 for coarse particles (D > 10 mm) and high-particle Reynolds numbers (Re > 400) as opposed to the value of 0.06. Given this assumed value for θ_{crit} Komar (1987a) modified equation II-18 by substitution into equation II-15 to account for a natural bed composed of a mixture of particle sizes resulting in the following equation

$$\tau_{crit} = 0.045(\rho_s - \rho_w) g D_{50}^{0.6} D_{\max}^{0.4} \qquad \text{(II-19)}$$

where D_{50} is the mean particle diameter and D_{max} is the maximum diameter and the exponent coefficient values 0.6 and 0.4 come from data where $D_{\max}/D_{50} \leq 22$. This re-formatted Shields entrainment function is a flow competence form; hence the substitution of D_{max} for D_i. It is also important to keep in mind that these empirical values come from low gradient (channel slope <0.002 m/m) data sets where the range in particle diameter was 10 to 100 mm (Fig. II-2). Extending equation II-19 to higher-gradient channels (channel slope >0.002) typically characterized by particle diameters approaching 1 m may produce serious errors.

The assumption that θ_{crit} approaches a constant value of 0.045 may not hold for larger values of the ratio $D_{\max}/D_{50} \geq 22$ (Komar, 1987a, 1988; and 1989). Andrews (1984) found a mean θ_{crit} value of 0.031 for gravel-bed rivers where the mean diameter was 23 mm to 120 mm. Andrews (1983) and others have argued that θ_{crit} will approach a minimum value of 0.02 for threshold entrainment in gravel-bed rivers. However, Carling (1983) found values for θ_{crit} as low as 0.006 by introducing large ($D_{\max}/D_{50} \approx 22$) tagged

boulders to a flowing stream. Novak and Nalluri (1975 and 1984) in flume experiments found θ_{crit} values as low as 0.004 by systematically introducing larger particles ($D_{max}/D_{50} \approx 80$) to a fixed bed of uniform sizes.

However, determining a θ_{crit} value by introducing a particle that is much larger than the underlying bed may be an invalid test that θ_{crit} can reach lower values than the minimum of 0.02 reported by Andrews (1983) where all measured particles were entrained from the bed. Moreover, all of the data that produced very low values for θ_{crit} come from small streams and flumes as opposed to the data of Andrews (1983) working in rivers where both channel dimensions and particle sizes were orders of magnitude greater. Data on θ_{crit} from steep gradient cobble and boulder rivers are non-existent; therefore, the limiting value of 0.02 reported by Andrews (1983) remains as a best estimate for river conditions. Lower values would be more appropriate for work in flumes and small streams like Oak Creek (Komar, 1987a) and Great Eggleshope Beck (Carling, 1983).

Particle shape, size and factors of packing control the effective pivoting angle and the particle surface area exposed to the flow. Numerous authors have postulated that a stream or river bed composed of a mixture of sizes and shapes would naturally lead to the situation where increased shear stress is necessary for threshold entrainment as compared to the situation of uniform particle size due to pivoting constraints (Komar and Li, 1986; Li and Komar, 1986; Komar 1987a&b; 1988; 1989; Hassan and Reid, 1990; Kirchner et al., 1990; Bridge, 1992; Carling, 1992). However, using data from natural beds lead to the reformatted Shields entrainment relation equation II-19 and the reported values for the *a* and *b* coefficients (Komar, 1987a&b; 1988; 1989). It is clear from the plotted comparison of flow competence relations that the reformatted Shields line lies below the theoretical Shields relationship for uniform particle sizes (Fig. II-2). The empirical analysis of (Komar, 1987a&b; 1988; 1989) demonstrates that having a mixed bed actually lowers the required shear stress compared to the situation of uniform grains (Fig. II-2).

It can be seen from equation II-5 that maximum shear stress can be expected to occur when the hydraulic radius, R, reaches a maximum at bank-full conditions. When flows increase and extend into the into the adjacent flood plain, wetted perimeter rapidly increases and limits increases of hydraulic radius. Bank-full conditions also produce maximum flow velocities and minimum flow resistance by similar argument, resulting in maximum shear stress as expressed in equation II-8. It follows that maximum shear stress during bank-full flow conditions should be sufficient to entrain the coarsest material. Therefore, flow competence estimates of shear stress based on the maximum and mean particle diameters from a channel using equation II-19 should be close to estimates of the maximum shear stress that can be produced in that channel using equation II-8. A data set from New Zealand is used to test this hypothesis.

BANK -FULL SHEAR STRESS VERSUS FLOW COMPETENCE

New Zealand Data Set

Hicks and Mason (1991) provide data on Manning and Chezy friction coefficients for New Zealand rivers. Physical and hydraulic characteristics were measured for 78 river reaches. Native bio-diversity is maximum in Montane and Piedmont valley flood plains and these geomorphologic habitats are typified by gravel and cobble alluvium (Stanford et al., 1996). A clear relationship exists between channel slope and substrate size, with gravel and cobble alluvial channels typically existing as high-gradient slopes. Therefore. a subset of 33 high-gradient sites were selected based on a slope criteria (slope >0.002 m/m after Jarrett, 1984) and used in the following flood analysis. Each selected site also had data on the particle size distribution of the surface bed material corresponding to the maximum, mean and D_{84}, sizes (the later is the size such that 84 % of the particles are smaller). The Chezy friction coefficient was calculated for each site over a wide range of flow conditions. On average, each site was visited six times and hydraulic data (i.e.

discharge, mean velocity, hydraulic radius) were measured. This resulted in 211 measures of flow velocity and discharge with some measurements made at flows approaching bank-full condition for the 33 sites. Complete details of all measured data can be found in the handbook *Roughness Characteristics of New Zealand Rivers* (Hicks and Mason, 1991). The particle size data were used to estimate actual shear stress with equation II-19. The hydraulic data were used here to estimate bank-full shear stress for each site with equation II-8.

Determining Bank-Full Discharge

Hicks and Mason (1991) provide plots of river cross-sections for all sites and define the range of water depth associated with discharge during their field measures. The data show that for most sites the maximum measured discharge nearly reached a level where for any further increase in discharge the top width of the channel would greatly increase relative to the cross-sectional area of the main channel defining a near bank-full condition. Williams (1978) examined measures of bank-full discharge from 233 gauged sites representing a wide variety of climatic and geographic conditions. He used a step-forward multiple regression technique to determine the following equation

$$Q_b = 4.0 A_b^{1.21} S^{0.28} \qquad \text{(II-20)}$$

where A_b is the cross-sectional area in square meters at bank-full discharge and S is the channel slope. The regression coefficients are significant at the 99% confidence level (Williams, 1978). Cross-sectional area was given for 33 New Zealand sites at maximum measured discharge, as well as, graphs of surveyed channel cross-sections showing the corresponding water level. The difference in elevation between the water level in the channel cross-sections corresponding to maximum measured discharge and the survey level of the bank top was estimated here from the graphs of the channel cross-sections. This elevation difference was multiplied by the maximum width, producing an estimate of the additional area above maximum measured discharge area. The sum of these two areas

resulted in a value for the cross-sectional area at bank-full discharge, A_b, greater than the actual area given that the bank geometry was ignored. The slope of the channel was taken as the maximum water surface level measured for each site.

Determining Bank-Full Mean Velocity and the Darcy-Weisbach Friction Factor

The ultimate quantity of interest is the shear stress associated with a bank-full discharge, given that shear stress would be near its maximum value under such conditions. To determine the shear stress for each site with equation II-8 a regression analysis was made between measured discharge, Q, velocity, U, and the Darcy-Weisbach friction factor, f_r, for all 211 measured flow conditions (Fig. II-3). The wide variance in f_r relative to discharge is related to the decreasing flow resistance at each site with increasing discharge (Fig. II-3). The estimated shear stress from these data incorporate all the variance associated with each site.

The regression coefficients from the measured hydraulic data are used to predict mean velocity and the Darcy-Weisbach friction factor for the estimated bank-full discharges with the following equations

$$U_b = 0.47 Q_b^{0.33} \tag{II-21}$$

and

$$f_{rb} = 0.76 Q_b^{-0.44} \ . \tag{II-22}$$

The reported error for these equations (Fig. II-3) were determined from confidence intervals at a 95% significance level. The values from these equations are then used to estimate the associated flow shear stress for the bank-full discharge at each site with the use of equation II-19. However, they could also be used to evaluate any flood condition for these sites.

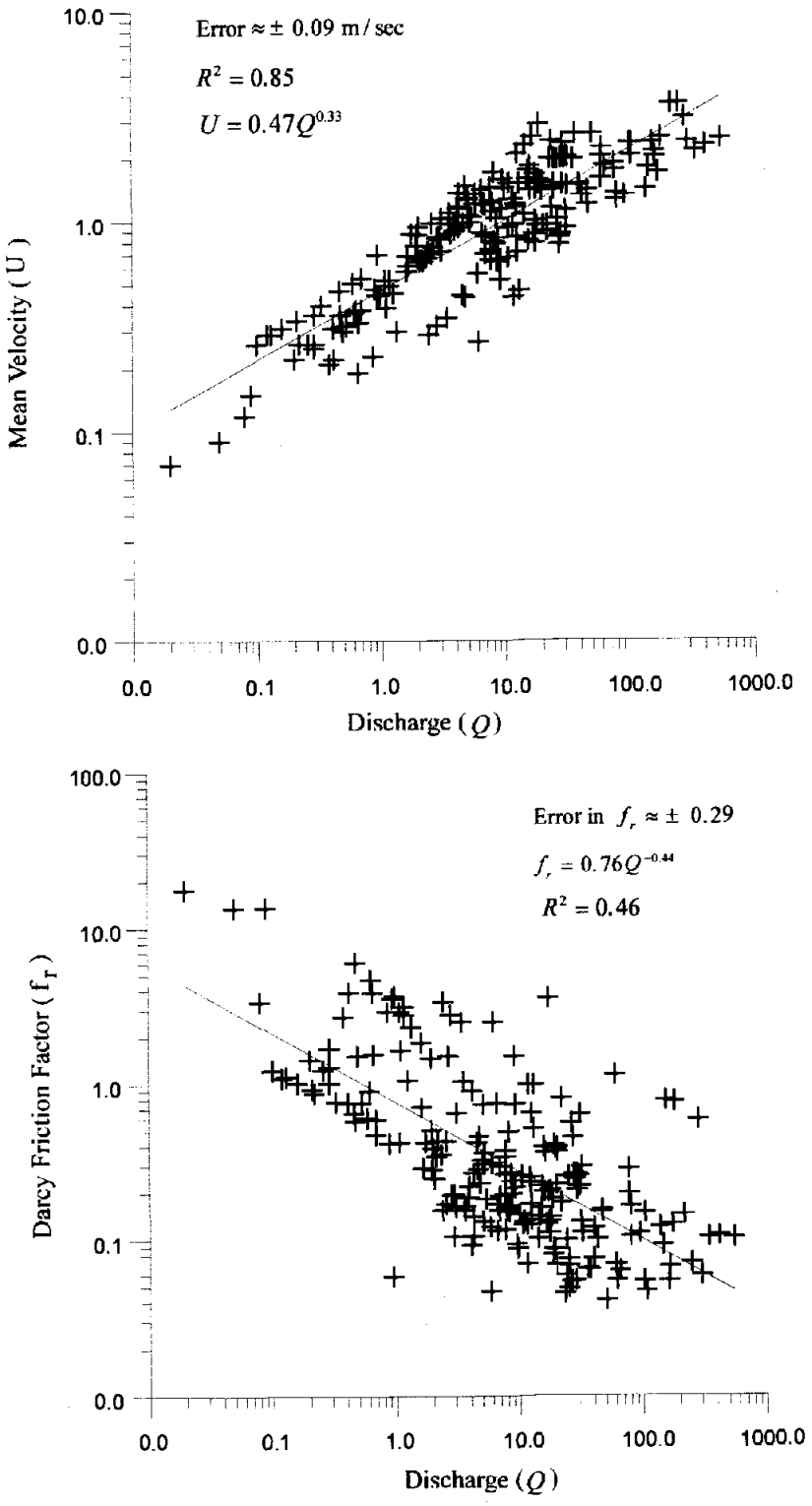

Figure II-3. The correlation between mean discharge and mean velocity (top) and between discharge and the Darcy-Weisbach friction factor (bottom). Mean velocity was determined with current meters.

Bank-Full Shear Stress Versus Substratum-Derived Flow Competence

Given the particle diameter data and utilizing the re-formatted Shields equation II-19, an estimate was made of the flow competence level necessary to achieve threshold entrainment for the complete range of particle sizes for each site. The question of interest is whether bank-full flow is sufficient to achieve threshold entrainment for all particles composing the bed. That question is addressed by comparing the ratio between the estimated bank-full shear stress, τ_b, and the substratum-derived critical shear stress, τ_{crit}, referred to as the mobility ratio, τ_b/τ_{crit}. When the mobility ratio, τ_b/τ_{crit}, equals unity, or higher, then theoretically threshold entrainment for the full range particle sizes composing the bed material has been achieved.

The mobility ratio, τ_b/τ_{crit}, plotted against the D_{84} particle size shows that bank-full discharge is a competent flow for six sites composed of gravel to cobble size bed material (Fig. II-4). As the bed material becomes coarser the ability of the bank-full shear stress to reach critical threshold entrainment levels decreases (Fig. II-4). Most sites have an approximate value of 0.45 or greater for the mobility ratio, τ_b/τ_{crit}. If the minimum value for θ_{crit} of 0.02 reported by Andrews (1983) where used in equation II-19 then most of the sites would reach $\tau_b/\tau_{crit} = 1$ or critical threshold during bank-full flow (Fig. II-4). Andrews (1984), working in gravel bed rivers with particle sizes where the median size ranged from 23 mm to 120 mm, found that bank-full shear stress exceeded the threshold value for entrainment of the median particle diameter of the bed surface when $\theta_{crit} = 0.02$. Andrews (1984) also reports that in 15 of the 24 sites examined that bank-full shear stress did not reach critical threshold levels for the coarse 10% of the bed.

Certainly much of the scatter in the comparison between the mobility ratio and particle size is due to the error in estimating mean velocity and Darcy-Weisbach friction coefficient for bank-full conditions (Fig. II-4). That error associated with the regression equations II-21 and II-22 translates into plus or minus error of about 0.2 for the mobility

ratio, τ_b/τ_{crit}, and is plotted as an error bar (Fig. II-4). However, the trend of lower mobility values for increasing particle size would still exist.

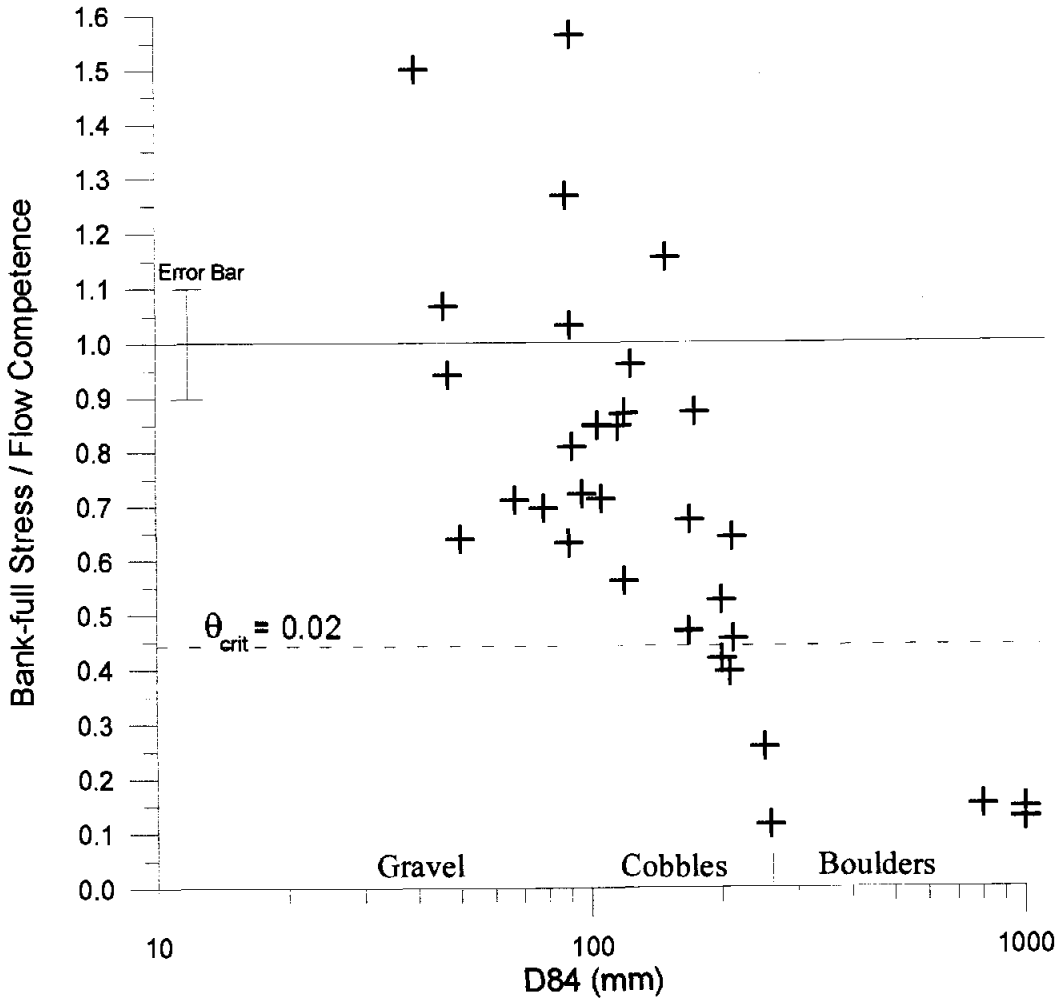

Figure II-4. Comparisons of the mobility potential, τ_b/τ_{crit}, of bank-full flow expressed as a ratio between bank-full shear stress, $\tau_b = 1/8 f_r \rho_w U^2$, and the reformatted Shields relation written as a flow competence equation for critical shear stress, $\tau_{crit} = \theta_{crit}(\rho_s - \rho_w) g D_{50}^{0.6} D_{max}^{0.4}$, with the D_{84} particle diameter.

Equation II-19 should be applied only when the ratio $D_{max}/D_{50} \leq 22$ (Komar, 1989). The mobility ratio plotted against the ratio D_{max}/D_{50} shows that all data used here fell within this accepted range (Fig. II-5). An argument could be made that a lower value for θ_{crit} should be used for higher values of D_{max}/D_{50}. However, if that argument is

valid than one would expect decreasing mobility ratios when a constant $\theta_{crit} = 0.045$ value is used in equation II-19. No such trend of a decreasing mobility ratio, τ_b/τ_{crit}, with increasing D_{max}/D_{50} exists (Fig. II-5). On the contrary the lowest mobility ratio occurs over a range in D_{max}/D_{50} from 3.8 to 16 (Fig. II-5).

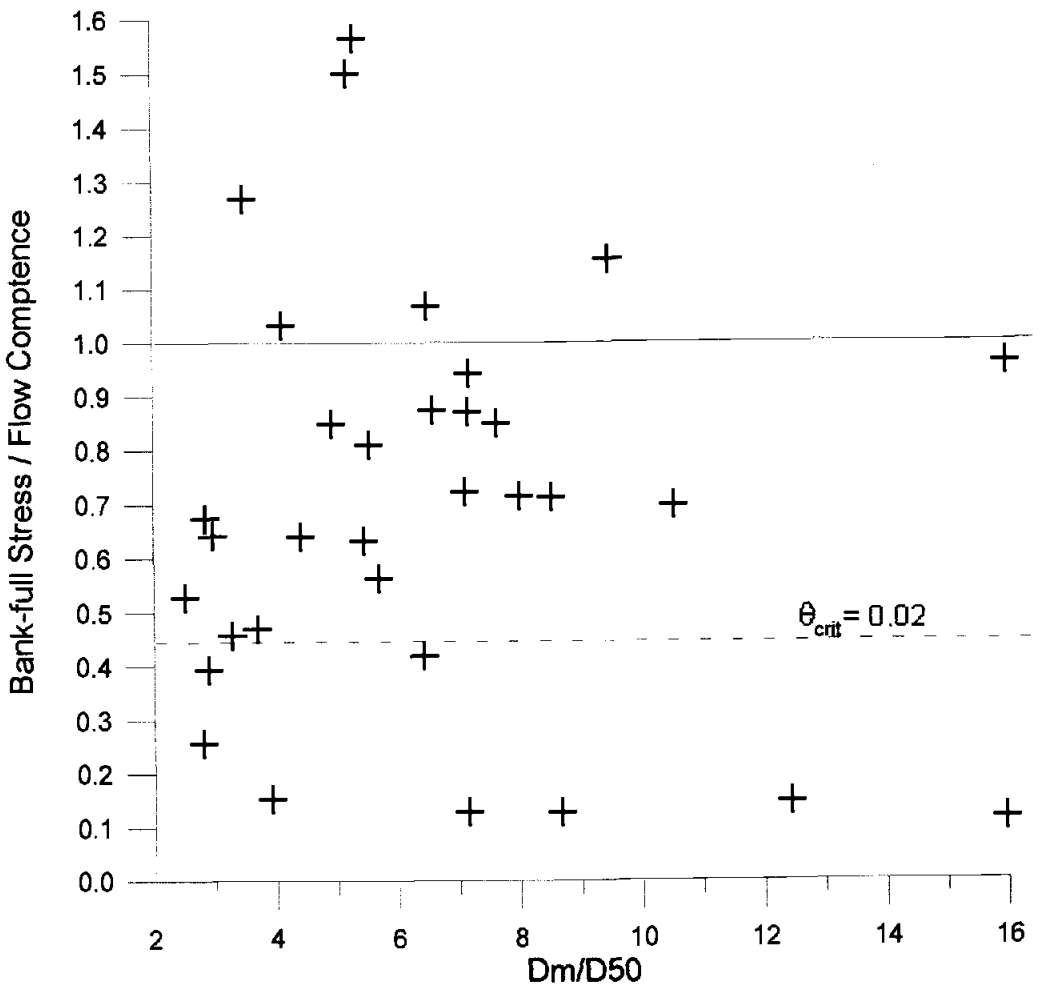

Figure II-5. Comparisons of the mobility potential, τ_b/τ_{crit}, of bank-full flow expressed as a ratio between bank-full shear stress, $\tau_b = 1/8 f_r \rho_w U^2$, and the reformatted Shields relation written as a flow competence equation for critical shear stress, $\tau_{crit} = \theta_{crit}(\rho_s - \rho_w) g D_{50}^{0.6} D_{max}^{0.4}$, with the ratio D_m / D_{50} where Dm is the maximum particle size and D_{50} the mean.

DISCUSSION

The reformatted Shields equation II-19 attempts to account for differences among empirical flow competence equations (Fig. II-2) by incorporating the mean and maximum particle diameters. Komar (1987a) showed that a bed composed of a mixture of particle sizes results in selective entrainment due to different pivoting angles. For a mixed bed, the condition exists where the pivoting angle, ϕ_1, for a small particle is greater then the pivoting angle, ϕ_2, for a larger particle (Fig. II-6). This results in different threshold stress requirements for each particle from those conditions for a bed composed of uniform-size particles.

Comparing the bank-full shear stress equation, II-8, to the critical threshold stress using equation II-19 shows a clear trend of decreasing mobility ratio as the distribution of particles becomes more coarse (Fig. II-4). Given the possible sources of error in estimating bank-full shear stress and in choosing the proper choice for θ_{crit} this trend indicates that equation II-19 over estimates critical entrainment threshold levels for coarse cobble and boulder bed rivers. Furthermore, assuming that θ_{crit}= 0.045 as indicted by the analysis of Komar (1987a and 1989) is the best estimate and that errors in estimating f_r decrease at higher flows as flow resistance decreases, then one could make the argument that equation II-19 over predicts critical shear stress by an order of magnitude. Given the fact that these channels do contain large rounded cobbles and boulders indicates that the flood flows experienced by the channels do in fact entrain these coarse particles.

Threshold entrainment results from the interaction between fluctuating shear stress close to the bed related to turbulent flow and the susceptibility of the particles to movement. When mean flow velocity increases the distribution of instantaneous flow stresses produced by the turbulence also increases. The initiation of particle motion involves instantaneous flow velocities and shear stresses rather than mean values of those fluctuating parameters. Therefore, some of the variance in the mobility ratio must be related to differences in level of turbulence in the flow field.

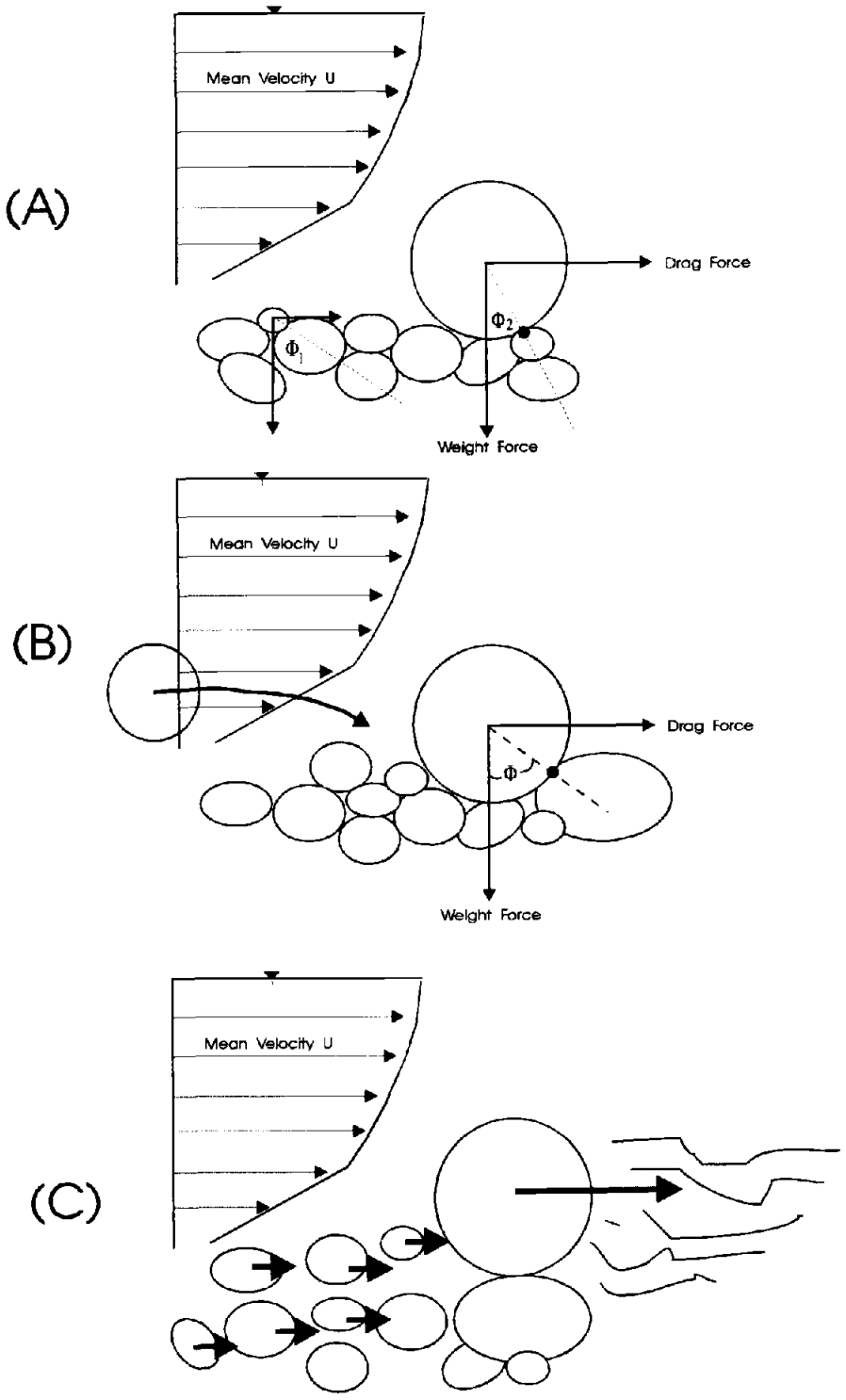

Figure II-6. Schematic comparison of the threshold entrainment condition due to different pivoting angles (A), the introduction of an entrained particle (B), and a fully mobile bed (C).

Momentum transfer between entrained particles and those held to the bed is another factor that is not accounted for in estimates of critical threshold entrainment. Clearly, the collisions between entrained particles and the bed would increase the ability of a flow to transport a larger particles than that predicted by equation II-19. The conventional approach of critical threshold entrainment assumes that there is no interaction with entrained particles coming from upstream, which requires homogenous pivoting relations throughout the stream reach (Fig. II-6A). If we assume that different pivoting angle constraints exist upstream for the same instant in time, or localized bed scour or bank erosion, then it is possible to introduce a saltating particle from upstream (Fig. II-6B) to our initially stable condition (Fig. II-6A). With this assumption of the presence of saltating particles, it is plausible to expect a change from an initially stable bed (Fig. II-6A) to a partially mobile or fully mobile bed (Fig. II-6C) at a mean flow velocity below the theoretical Shields threshold criteria for the largest river-bed particles.

The momentum transferred from entrained particles to those at rest could become a physical process of key significance if the particles at rest are subject to flow stresses close to their entrainment threshold condition. The net effect would be mobilization of the entire bed at velocity levels below the threshold criteria given by theory that does not include that process. Indeed, field studies of threshold entrainment have reported particle velocities greater than mean flow velocities and simultaneous bursts of many particles below theoretical threshold criteria (Hammond et al., 1984 and Drake et al., 1988). Moreover, the empirical analysis that leads to the reformatted Shields relation (equation II-19) suggests that a mixed bed results a lowering of the critical threshold curve (Fig. II-2). This only makes sense given that a mixed bed would not only produce situations of sheltering and higher pivoting angles, but also the converse situation of larger particles more exposed to the flow and with reduced pivoting angles. Indeed, the data of Carling (1983) and Hammond et al. (1984) resulted in a lower slopes than the theoretical Shields curve (Fig. II-2).

CONCLUSIONS

The concept of flow competence depends on a relationship between threshold shear stress and particle diameter where the size of the maximum entrained particle infers a measure of the shear stress. The Shields entrainment relation has been re-written into a flow competence equation, II-19, dependent on both the mean, D_{50}, and maximum, D_{max}, particle diameter assuming a constant value for the Shields entrainment function, θ_{crit} (Komar, 1987a; 1988; 1989). This reformatted Shields equation was used to examine the flow competence level of bank-full flow for 33 steep-gradient river reaches with river bed particles ranging in size from gravel to boulders. As the bed material becomes coarser the ability of the bank-full shear stress to reach critical threshold entrainment levels decreases (Fig. II-4). Furthermore, nearly an order of magnitude increase in shear stress would be necessary to entrain boulder size substratum (Fig. II-4). Increasing discharge above bank-full conditions would for the most part only cause inundation as the flood waters over top the bank. This would not theoretically cause a sufficient increase in shear stress.

The reformatted Shields relation, equation II-19, does not take into account collisions between particles. This process would transfer momentum more efficiently to the bed than a clear flow, and thereby, entrain larger grains than expected from only the fluid shear stress. Therefore, it is postulated that the extension of the reformatted Shields equation to flood deposits and boulder-bed rivers could over-estimate hydraulic conditions.

CHAPTER 3

PREDICTING THRESHOLD ENTRAINMENT AND STABLE BOULDER MASS FOR A BEACH

ABSTRACT

The critical threshold mass for boulders composing a beach is the mass of the largest stone entrained by the hydraulic forces associated with wave breaking and swash run-up. For any given storm event there is a maximum boulder mass that can be moved and another slightly larger boulder that has the minimum mass necessary to remain stable. Two equations are derived: one to estimate critical threshold mass and another to estimate minimum stable mass for boulders on a beach. Both equations include the same physical parameters: stone density, beach slope, breaking wave height, water depth, wave period, run-up height, maximum swash velocity and average swash velocity. In both equations the wave force applied to the beach face is scaled relative to the elevation that wave energy raises the water surface. Scaling the wave force relative to the run-up elevation results in a critical threshold formula. This is given as equation III-41. Its predictions accurately match field data giving the largest boulder transported on a beach during storm events. Scaling the wave force relative to the breaking wave height results in a stability formula. This is given as equation III-42. It predicts stable stone mass in the range defined by the Hudson formula. Equation III-42 has the advantage over the Hudson formula by incorporating the physically important parameters of wave period and swash velocity into a practical expression without having to account for these factors by guessing the proper value for an empirical stability coefficient. Both equations could be useful in the initial evaluation and design of dynamic revetments constructed with quarry stone.

INTRODUCTION

Boulder Beaches

Boulder beaches are common features of many rocky coasts throughout the world. They generally form at the base of sea cliffs and provide a protective buffer against wave attack. In this context, boulder beaches represent the natural equivalent to a dynamic rubble revetment. Natural boulder beaches deform in profile relative to changing storm wave conditions, but maintain a general dynamic equilibrium slope (Oak, 1981; 1985). The profile deforms in response to the transport of boulders composing the beach. Oak (1981) found that boulder entrainment occurred only during storms and that initial displacement was in direct response to wave breaking and up rush of the wave swash. The main role of the backwash on a boulder beach is to remove finer material, thereby maintaining an armored beach face characterized by high porosity. These dynamic characteristics of a boulder beach provide a natural buffer from direct wave attack for the backshore environment of a sea cliff. The result is that sea cliffs, with boulder beaches developed at their toe, erode at very slow rates.

The ability to quantify the wave conditions that will initiate movement and transport of boulders is important for ecologists studying rocky coastlines. It is of equal importance for coastal engineers interested in mimicking the boulder beach behavior in the design of dynamic revetments constructed for shore protection.

Coastal Engineering Design

Over the last decade interest has turned towards the design of dynamic revetments that provide the necessary level of protection by allowing the structure to deform under wave attack (Pilarczyk and der Bor, 1983; van der Meer and Pilarczyk, 1986; Johnson, 1987; van der Meer, 1987 and 1988; Powell, 1988; Ahrens, 1990; Lorang, 1991; van der Meer, 1992; Silvester and Hsu, 1993). In this light, coastal engineers are designing with the intent to mimic the dynamic behavior of naturally occurring boulder, cobble and gravel

beaches. However, an equation does not exist that estimates the critical threshold mass for use in the design of dynamic revetments.

The most frequently used formula for breakwater and static shoreline revetment design is the Iribarren formula (1938), modified by Hudson (1952) and adopted as the Hudson formula by the Army Corps of Engineers in their Shore Protection Manual (SPM 1984). The Hudson formula gives estimates of individual stone mass necessary to construct a static shore protection structure in terms of wave height, structure slope and stone density. It is given as

$$W = \frac{\rho_s H_s^3}{K_D \left(\frac{\rho_s - \rho_w}{\rho_w} \right)^3 \cot \theta} \qquad \text{(III-1)}$$

where W is the minimum stable mass, H_S is the significant deep-water wave height or the significant wave height at the structure base, ρ_S and ρ_w are stone and water density, respectively, θ is angle the beach makes with the horizontal, and K_D is a stability coefficient empirically derived from wave tank studies (SPM, 1984). One can see from the equation that stone mass is mainly a function of the significant design wave height. Other wave parameters are ignored, such as, wave period, swash velocity or run-up height. Unfortunately, these are the physical parameters that describe wave action upon a shoreline revetment designed to provide protection against wave erosion.

In the case of estimates from the Hudson formula, waves smaller than the design height can damage a coastal structure, ranging from the transport of a few individual stones to complete failure of the structure (Ahrens and McCartney, 1975; Bruun and Gunbak, 1977; Ahrens, 1981). Such damage has been attributed in part to the affect wave period has on the hydraulic forces acting against a coastal structure (Bruun and Gunbak, 1977). An increase in wave period for any given wave height results in an increase in

wave power expended on the structure. One would intuitively expect the corresponding entrainment of increasingly larger stones. The fact that wave period is not included in the Hudson formula has been sited as a short coming in its use as a design tool (Hudson, 1952; Bruun and Gunbak, 1977).

The Army Corps of Engineers responded to this short-coming in the theoretical development of the Hudson formula with numerous wave tank studies aimed at finding values for the stability coefficient, K_D, that accounted for stability through interlocking structure units or special placement of stones (Hudson, 1952; SPM, 1984). When estimating stable stone mass, the typical design procedure is to consult the tables presented in the SPM and choose the proper K_D value that corresponds with the structure material, mode of placement, morphology (i.e. structure head or trunk) and the expected form of wave breaking. The Hudson formula has been a useful tool in the design of static structures because it relies on readily attainable variables that result in an over-estimate of minimum stable stone mass, thereby providing an adequate level of design safety. However, a similar formula does not exist for the design of dynamic revetments and the designer is left with having to guess at values for the stability coefficient, K_D, that reflect the critical threshold entrainment condition from the Hudson formula.

ANALYSIS OF BOULDER ENTRAINMENT ON A BEACH

Descriptive Processes

Wave competence is a term used here that refers to the size of the largest entrained boulder as related to the wave hydraulics that caused the entrainment. The entrainment of boulders on a boulder beach is viewed as occurring during two regimes of wave energy. The first is a relatively low-wave energy regime that occurs during periods of low-wave height and long-wave period. For this regime, only a small portion of the boulders comprising the beach are selectively entrained. The main processes would be (1)

winnowing away of fine material, (2) some boulder rounding due to impact fragmentation, and (3) some boulder smoothing due to abrasion. The second regime occurs at a higher energy level associated with storm wave conditions. This high energy regime is characterized by a dynamic beach state where most, or all, of the boulders shift position or rock in place, with the smaller boulders perhaps being rolled over or pushed up-slope.

One might argue that during storms wave breaking on the beach face dislodges individual boulders that are then pushed up-beach by the swash. Bruun and Gunbak (1977) found that as swash velocity increased, large over-turning moments developed on the blocks composing a quarry-stone structure. The result was the initial movement of individual stones. Novak (1969) measured the size of the largest transported clast on a gravel beach and the velocity of the swash. The largest gravel clast transported had an intermediate particle diameter of 0.1 m and was transported by a swash velocity of 2.42 m/sec corresponding with a breaker height of 0.44 m. Therefore, swash velocity associated with even small waves (0.44 m) can produce turbulent flow sufficiently competent to entrain both the gravel and cobble components of the beach. Bagnold (1940) argued that the potential energy carried away by the water that percolates into the beach results in a situation where the return flow of the backwash will be a less competent flow then the up rush of the swash. Oak (1981) found that boulder displacement and transport occurred only during storms and that the initial motion was mainly in the up-beach direction.

The conclusion from the above discussion is that swash velocity must be used in the development of a wave-competence equation. The methods used to estimate wave transformation from deep water to run-up of wave swash and beach scaling follows. The assumptions and methods used to represent the drag coefficients that arise in the derivations are discussed below in terms of swash resistance as a function of beach roughness. And finally the relationship between increased wave power and the entrainment of increasingly larger boulders is introduced and referred to as wave competence where

the size of the largest entrained boulder reflects the wave hydraulics that caused the entrainment.

Wave Transformations and Beach Scaling

The transformation from deep water waves to final run-up, R_u, of wave swash on the beach face is a complex process that becomes increasingly so for a low sloping nearshore (Fig. III-1).

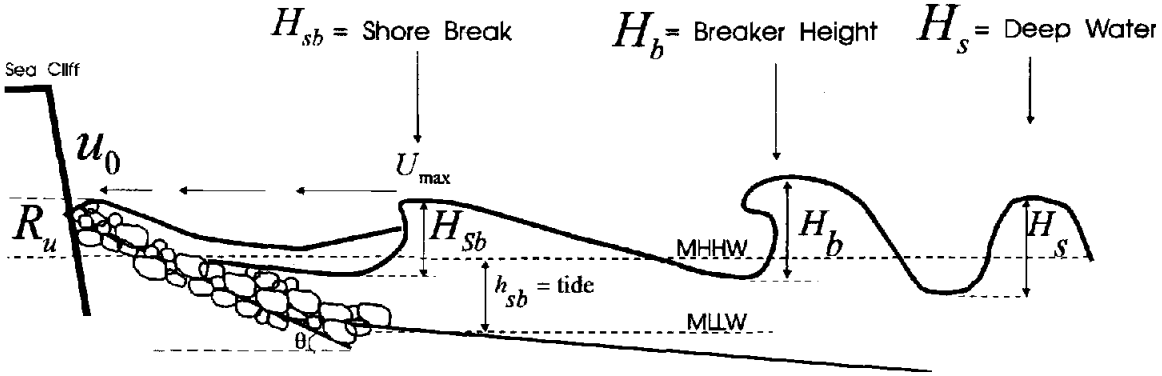

Figure III-1. Schematic of the process of wave transformation from an initial off-shore wave height to the final run-up of swash on the beach face.

As storm energy increases incident waves continually break further offshore producing a surf zone 100's of meters wide on low sloping sand beaches or wave cut terraces. These surf zones may have many bores between the break-point and final run-up. On many gravel, cobble and boulder beaches storm waves never reach the beach face during low tide. The energy is dissipated in the wide surf zone that exists at that tide level. In contrast, during high tide, and under similar storm intensity, waves initially break very near the beach face separated by maybe one or two surf bores (Fig. III-1). Estimating run-up elevation from offshore wave conditions is most reliable when wave breaking occurs close to the beach without a large intervening surf zone.

Wave run-up can be estimated from the deep water wave statistics and slope of the beach. Battjes (1974; a & b) modified the Hunt (1959) formula for the 2% run-up elevation, $R_{u2\%}$, by re-writing the equation in terms of a dimensionless surf similarity parameter, ξ, that he referred to as the Iribarren number. The expression

$$R_{u2\%} = C_r H_s \xi \qquad \text{(III-2)}$$

relates the run-up elevation to the Iribarren number, ξ, the deep water significant height, H_s, and an empirical constant C_r. The Iribarren number is a non-dimensional parameter that relates beach steepness to offshore wave steepness. It is an important scaling parameter when estimating run-up on a boulder beach or similar artificial rock slopes (Battjes, 1974a & b; Ahrens and McCartney, 1975; Ahrens, 1981; Allsop et.al., 1985; Holman, 1986; Dalrymple, 1992; Waal and van der Meer, 1992; van der Meer and Stam, 1992). The expression is

$$\xi = \frac{\tan\theta}{\sqrt{\frac{H_s}{L_o}}} \qquad \text{(III-3)}$$

where $\tan\theta$ is the slope of the beach and L_0 is the deep-water wave length. From linear wave theory we can derive an approximation for L_0, given as

$$L_o = \frac{1}{2\pi} g T^2 \qquad \text{(III-4)}$$

where T is the wave period and g is gravity. Substitution of III-4 into III-3 and III-3 into III-2 yields

$$R_{u2\%} = C_r \sqrt{\frac{g}{2\pi}} T \sqrt{H_S} (\tan\theta). \qquad \text{(III-5)}$$

Van der Meer and Stam (1992) found a value of 0.55 for C_r, corresponding to a range of $0.5 < \xi < 2$ due to irregular waves on porous rock slopes. They referred to C_r as the run-up attenuation constant and found that it depends on beach coarseness and permeability which attenuates the run-up through frictional resistance of the swash and loss of water. Holman (1986) also found similar values for C_r using measures of swash from a sand beach. For very steep boulder beaches as wave energy increases run-up elevation increases in a linear fashion at incident wave frequencies for the range of surf similarity parameters $\xi = 0.5>2.5$ (Holman, 1986; Kobuhisa N. et al. 1988; van der Meer and Stam, 1992). The data used in this thesis come from storm conditions where ξ fell within this range. Gravel and boulder beaches typically exist in these ranges for ξ. The fundamental physical principles between beach slope and wave steepness are related through the derivation of ξ. Therefore, the derivation of ξ follows below to show how those arguments are used to later describe swash deceleration.

We begin with a wave impinging on a gravel or boulder slope as a swash bore that collapses at the shore break and surges up the gravel beach face (Fig. III-1). This swash bore must decelerate from a maximum velocity, u_{max}, at the shore break position (equal to maximum run-down for monochromatic waves) to zero over a time interval ideally equal to 1/2 the wave period. We can approximate maximum velocity with the following

$$u_{\max} = \sqrt{gH_{sb}} \qquad \text{(III-6)}$$

where H_{sb} is the wave height at the shore break position. We can define a time interval t as

$$t = \frac{T}{2}. \qquad \text{(III-7)}$$

The deceleration, $\partial u/\partial$ of the swash equals the down slope component of gravity, $g \sin \theta$. This condition written for a sloping beach is

$$\frac{\partial u}{\partial t} = g \sin \theta \qquad \text{(III-8)}$$

where θ is the angle between the beach face and horizontal (Fig. III-1). We can now make the following approximation through substitution

$$\frac{\partial u}{\partial t} \approx \frac{\sqrt{gH_s}}{0.5T} = g \sin \theta \qquad \text{(III-9)}$$

where the substitution of H_S for H_{sb} is required to equate offshore wave steepness to beach slope as expressed in the Iribarren number. Solving for $\sin \theta$ and squaring both sides yields

$$(\sin \theta)^2 = \frac{H_s}{0.25gT^2}. \qquad \text{(III-10)}$$

solving III-4 for wave period yields

$$T^2 = L_0\left(\frac{2\pi}{g}\right) \qquad \text{(III-11)}$$

and substituting III-11 into III-10 yields

$$(\sin \theta)^2 = \frac{H_s}{0.25g\left(L_0 \frac{2\pi}{g}\right)} \qquad \text{(III-12)}$$

squaring both sides and rearranging as a ratio equal to some constant yields

$$\frac{\sin\theta}{\sqrt{\frac{H_s}{L_o}}} = \text{constant} \qquad \text{(III-13)}$$

where the constant is approximately the Iribarren number, ξ, related to wave steepness and beach slope expressed as $\sin\theta$.

Beach Roughness and Swash Resistance

Flow resistance, in a river, occurs in part because of bed roughness associated with particle size. Maximum roughness for a river channel occurs when particle diameter approaches flow depth (Van Rijn, 1982). By analog to a boulder beach, flow resistance of the swash up the beach face occurs in part due to the roughness associated with boulder size. The condition of maximum roughness occurs when boulder diameter equals run-up, R_u, or when the swash thickness equals the boulder diameter (Fig. III-2). This type of roughness scale becomes important when estimating the frictional drag between the beach face and the swash. The ratio used here to express average roughness of a boulder beach is

$$\frac{R_u}{D_{50}}, \qquad \text{(III-14)}$$

where D_{50} is the intermediate mean boulder diameter comprising the beach face.

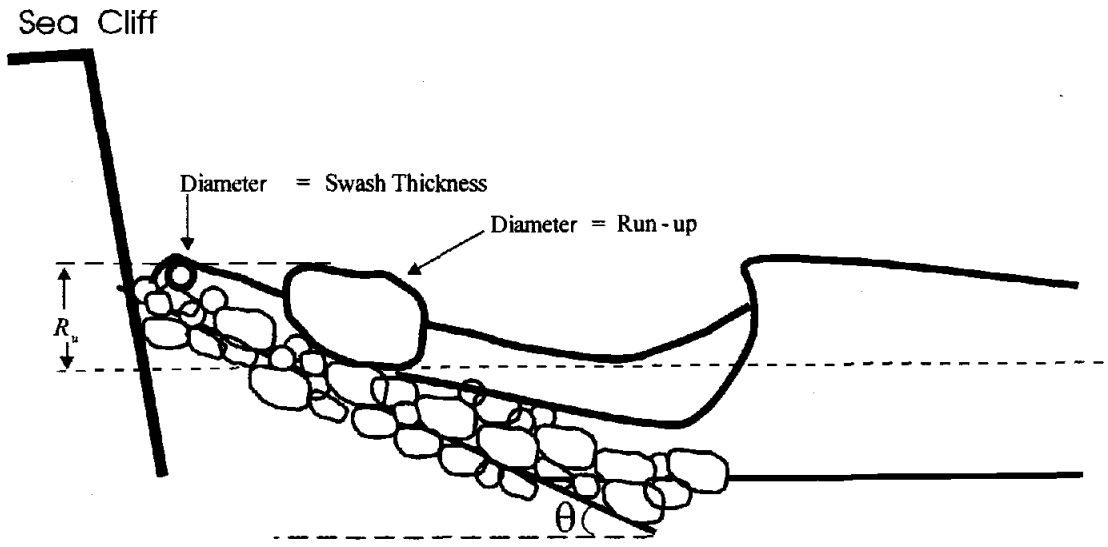

Figure III-2. Schematic diagram for two conditions of maximum roughness; one when boulder diameter equals run-up elevation and another when boulder diameter just equals swash thickness.

Hughes (1995) presents an equation for estimating the frictional resistance, f_r, associated with wave swash up a low sloping sand beach face

$$f_r = \frac{8}{\left(2.5\ln\left(30\frac{h_s}{k_s}\right)\right)^2} \qquad \text{(III-15)}$$

where h_S is the thickness of the swash at any point on the beach face and k_S relates to grain size. This expression is derived from arguments of boundary layer thickness for fully turbulent uniform flow. Hughes (1995) made the assumption that swash velocity on a low sloping sand beach can be approximated as steady state flow and that the roughness ratio should be adjusted when concerned with the friction caused by entrained sediment.

Similarly, an assumption is made that roughness scaled by the run-up height and boulder size modifies equation III-15 into a first-order expression for the frictional resistance, f_{BF}, between the swash and surface of a boulder beach. This is done through

substitution of equation III-14 for the roughness ratio, h_s/k_s, in equation III-15 and also assuming that f_r is a proportional to f_{BF} , thus yielding

$$f_{BF} = \frac{8}{\left(2.5\ln\left(30\frac{R_u}{D_{50}}\right)\right)^2}. \qquad \text{(III-16)}$$

Wave tank experiments have shown that frictional drag of wave swash ranges from 0.3 for rough angular rip rap to 0.05 or less for smooth cobble and boulder slopes (Kobushia and Greenwald, 1986; Kobushia et. al., 1988; Kobushia and Desilva, 1989). Under maximum roughness conditions equation III-16 gives a maximum value of 0.1 for f_{BF}. Data used from an Australian boulder beach gives a value of 0.03 for f_{BF} with equation III-16. This value is consistent with reported values from experimental work. Equation III-16 is used simply as an objective way of determining a value for the drag coefficient that appears in the following derivation for stress on the beach face. Improvements in the predictions from the critical threshold and stability equations derived would be expected given a better means of expressing frictional resistance. However, equation III-16 does give an objective estimate of frictional resistance within an expected range of published values and by using easily obtainable physical data. Therefore, it represents a best estimate at this time.

Wave Power and Wave Competence

Wave power represents the work available to entrain boulders composing a steep sloping beach. It is intuitive that wave power increases during storm conditions and that correspondingly larger boulders will be mobilized. The ability of waves to entrain boulders is referred to as wave competence and it is related to the available wave power. The shoreward energy flux in deep water, P_O, is

$$P_o = EC_g n \qquad \text{(III-17)}$$

where E is wave energy, C_g is the group velocity and n is a dimensionless coefficient that varies with depth equal to 0.5 in deep water and increasing to 1 as the wave shoals to the break point (Komar 1976). Wave energy E is given by

$$E = \tfrac{1}{8}\rho_w g H_s^2 \qquad \text{(III-18)}$$

where the group velocity C_g is given as

$$C_g = (g/4\pi)T \qquad \text{(III-19)}$$

From these expressions one can see that wave power at the shore break, P_{sb}, directly seaward of the beach face (Fig. III-1), can be expressed as

$$P_{sb} = \text{Constant} * H_{sb}^{\ 2} T \qquad \text{(III-20)}$$

where H_{sb} is the height of the breaking wave (Fig. III-3). Increasing the wave period for any given wave height at the shore break position would increase the wave power available to mobilize boulders on a beach (a point made earlier in discussing the limitations of the Hudson formula).

Swash velocity is important for threshold entrainment. However, the movement of boulders during storms occurs in response to other hydraulic complexities associated with wave breaking and swash run-up. These complexities arise from factors such as: dynamic pressure forces directly related to breaking waves, flow deceleration of the swash, and internal head pressure within the beach matrix due to percolation. The approach taken here is that the hydraulic forces active during storms are best represented by the wave

height at the shore break position, H_{sb}, wave period, T, run-up elevation of the wave swash, R_u, and estimates of maximum and average swash velocities, U_{max} and U_{avg}, respectively (Fig. III-3). The height of the breaker directly impinging the beach face, H_{sb}, is analogous to engineering specifications that require determining wave height at the base of the structure. Wave height at the shore break, H_{sb}, is depth dependent and can be estimated from the tide elevation above mean low water level. This is possible given that the toe of a boulder or gravel beach typically coincides with elevation of the low tide terrace (Nichols, 1988 and 1990) and data gathered for this thesis.

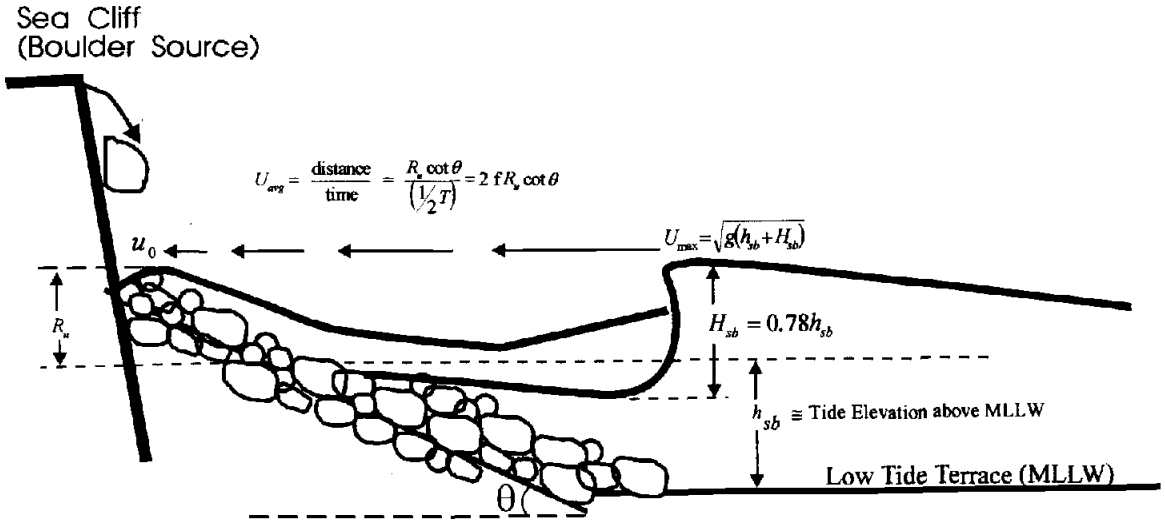

Figure III-3. Schematic depiction of wave collapse at the shore break position followed by swash run-up on a boulder beach showing variables used to determine boulder entrainment and stability. The low tide terrace typically corresponds to the mean low tide level given here as mean lower low water (MLLW) for a mixed semi-diurnal tide.

FORMULA DERIVATION

Defining Fluid Stress on the Beach Face

For any environment the fluid force acting on a potentially mobile bed is the first quantity of interest when evaluating threshold entrainment. For a steady-state turbulent flow the boundary shear stress, τ, is proportional to the fluid density and the square of the mean velocity U:

$$\tau \propto \rho_w U^2 \qquad \text{(III-21)}$$

(Henderson, 1966; Sternberg, 1972; Yalin and Karahan, 1979). Shear stress between a uniform turbulent flow and a potentially mobile bed can be derived from arguments of conservation of momentum yielding

$$\tau = f_r \rho_w U^2 \qquad \text{(III-22)}$$

where f_r is a friction coefficient that refers to flow drag associated with bed roughness as water flows through a channel. This expression relates the time-averaged mean velocity near the bed to the force exerted by the fluid.

Wave swash up the beach face is not a steady-state flow but rather a decelerating flow. Therefore, in order to apply equation III-22 a modification for this non-steady condition is needed. The first step is to separate and define two velocity terms; the maximum swash velocity, U_{max}, and the average swash velocity, U_{avg}. The second step is to substitute them into an expression for fluid stress more representative of the non-steady state flow conditions of wave swash.

The maximum swash velocity, U_{max}, in shallow water is equal to the wave velocity at the shore break and is related to the depth of water, h_{sb}, plus the breaking wave height, H_{sb}, in the following manner

$$U_{\max} = \sqrt{g*(h_{sb} + H_{sb})}. \qquad \text{(III-23)}$$

Ideally, swash velocity decreases from this maximum at the break point to zero at the maximum run-up elevation, R_u (Fig. III- 3). Over the intervening distance, water percolates into the beach matrix as the swash momentum decreases resulting in a seaward flowing backwash after complete run-up.

The average swash velocity, U_{avg} , is used to represent swash deceleration as a function of wave period and beach slope. This is done by dividing the horizontal excursion distance of the run-up by the time it takes the swash to decelerate across that distance (Fig. III-3). This deceleration occurs over a time period, t, ideally equal to 1/2 of the wave period, T, and the horizontal excursion distance, X, is defined by the run-up elevation and beach slope geometrically as

$$X = R_u * \cot\theta. \qquad \text{(III-24)}$$

The average velocity follows from substitution as

$$U_{avg} = \frac{X}{t} = \frac{R_u \cot\theta}{\left(\frac{1}{2}T\right)} = R_u 2\mathrm{f}\cot\theta \qquad \text{(III-25)}$$

where, $\mathrm{f} = \frac{1}{T}$ is the swash frequency.

Equation III-22 can be used as a starting point to make a first-order approximation of fluid stress applied to the beach face, τ_{BF}, by substituting the product of maximum swash velocity, U_{max}, and the average velocity, U_{avg}, of the run-up for U^2 in the following manner

$$\tau_{BF} = f_{BF}\rho_w |U_{\max}||U_{avg}| \qquad \text{(III-26)}$$

where f_{BF} represents flow drag between the beach face and the wave swash equation III-16. This approach treats stress applied to the beach face by wave swash as a function of the wave period, maximum and average swash velocities, run-up elevation, and slope. Substitution of equation III-23 and equation III-25 into equation III-26 yields

$$\tau_{BF} = f_{BF}\rho_w U_{\max} R_u 2\mathrm{f}\cot\theta \qquad \text{(III-27)}$$

where τ_{BF} is dimensionally consistent with τ, equation III-22, for turbulent fluid stress in rivers.

In contrast with a river, the non-steady-state flow condition that characterizes the beach environment is addressed by separating the velocity squared term in equation III-22 into two components, U_{max}, and U_{avg}. The assumption is made that the U_{max} term represents the initial turbulent portion of wave up-rush that gives the swash its initial impetus to travel up the beach face. The U_{avg} term represents the "energy-depletion" portion of the turbulent flow of wave swash up the beach face. During this phase the flow velocity of the swash decelerates in response to gravity, frictional resistance due to surface roughness and momentum lost to percolation. This aspect of swash deceleration enters the derivation through the dependence of U_{avg} on run-up elevation, beach slope and swash frequency equation III-22. Expressing stress in this manner modifies the steady-state turbulent flow expression, III-22, into a non- steady-state expression, III-27, applicable to at least first-order for stress applied to the beach face. The assumptions made above incorporate how far wave swash runs up the beach versus how long it takes to get there, equation III-25, into a dimensionally correct expression of the stress between the swash and the beach face, equation III-27.

Force Balance Considerations

The immersed weight of each boulder, F_{iwt}, is the force that holds it to the beach against the wave forces associated with wave collapse and swash run-up (Fig. III-4). The maximum boulder mass, m, that can be entrained by the wave force comes from the definition of the immersed weight force, F_{iwt}, in the following manner

$$F_{iwt} = (\rho_s - \rho_w) g \frac{m}{\rho_s}. \qquad \text{(III-28)}$$

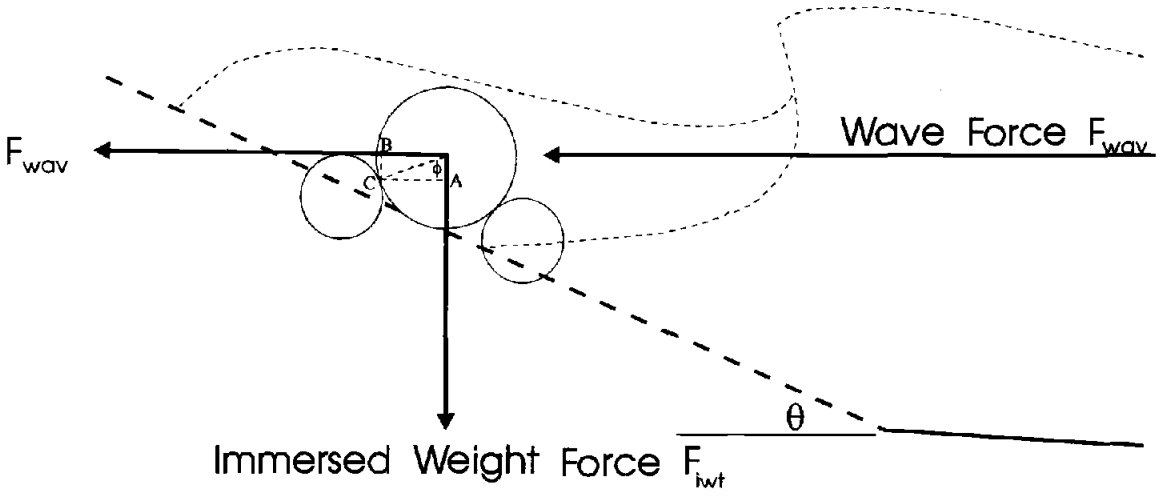

Figure III-4. Schematic depicting the relationship between the wave force, F_{wav}, trying to push a spherical boulder into the beach and the weight force, F_{iwt}, acting to hold the boulder in place. The angle ϕ reflects the pivoting angle with a nearly spherical boulder about the contact point C.

The flow trajectories of the water comprising the wave are initially directed into the beach and then forced in the up slope direction as wave swash. Likewise, the force of the wave initially tries to push the boulders horizontally in the direction of wave propagation; however, entrainment occurs with the swash in the up-beach direction (Fig. III-4). To describe this relationship, the scalar value of the entraining wave force can be expressed as

$$|F_{wav}| = \tau_{BF} * l^2 \qquad \text{(III-29)}$$

where l is a length scale. An assumption is made here that l^2 corresponds to a vertical projection area of the beach face exposed to the available wave energy, rather than the surface area of an individual boulder.

The overall goal is to relate increased wave energy or power to the entrainment of larger boulders. This wave competence argument requires that the total wave force be scaled according to some factor related to wave energy. Maximum wave energy at the shore break is expressed as

$$E_{H_{sb}} = \tfrac{1}{8}\rho_w g H_{sb}^2 \qquad \text{(III-30)}$$

and the remaining energy on the beach face can be approximated by the run-up elevation in the following manner

$$E_{R_u} = \tfrac{1}{8}\rho_w g R_u^2. \qquad \text{(III-31)}$$

For the condition of critical threshold entrainment, the projection surface area of the beach exposed to the available wave energy is scaled by defining l equal to R_u resulting in

$$|F_{wav}| = \tau_{BF} * R_u^{\,2} \qquad \text{(III-32)}$$

and substitution of equation III-27 into equation III-29 yields

$$|F_{wav}| = f_{BF}\rho_w U_{\max} R_u^3 2\mathrm{f} \cot\theta. \qquad \text{(III-33)}$$

Substitution of run-up elevation, R_u, or wave height, H_{sb}, at the shore break in equation III-29 appropriately scales the wave force relative to the available wave energy. The result of scaling in this manner is that the wave force increases with increasing wave energy. Consequently, the final wave competence equation derived below predicts increasingly larger boulders with increasing wave energy. This desired result would not occur it the wave force was scaled relative to the surface area of a boulder. Therefore, scaling the wave force relative to the elevation that the wave energy raises the water surface is a necessary assumption. Boulder surface area enters the equation as part of a coefficient in the derivation below. Further development of a critical threshold entrainment equation for boulders on a beach follows that of the Shields entrainment function for critical threshold entrainment in rivers.

Critical Threshold Entrainment

Critical threshold entrainment for any boulder on the beach face occurs when the moment of the wave force, F_{wav}, about the pivot point C equals the moment of the weight force, F_{wt},

$$F_{wt} * \overline{AC} = |F_{wav}| * \overline{BC} \qquad \text{(III-34)}$$

where

$$\overline{AC} = \left(\frac{D}{2}\sin\phi\right) \text{ and } \overline{BC} = \left(\frac{D}{2}\cos\phi\right) \qquad \text{(III-35)}$$

and D is the diameter of the sphere (Fig. III-4). The wave force only acts against the exposed projected surface area of the boulder, which is a function of size, shape and

packing arrangements of the boulders composing the beach. Therefore, the wave force of equation III-32 can be modified to account for these factors in the following manner

$$|F_{wav}| = \tau_{BF} * R_u^2 * \left(\frac{\alpha_1}{C_p} \right) \qquad \text{(III-36)}$$

where α_1 is a shape factor and C_p is a packing coefficient that together describe the projection surface area exposed to the wave force. Critical threshold entrainment occurs when the wave force equals the weight force

$$F_{wt} = |F_{wav}|. \qquad \text{(III-37)}$$

Substitution of equations III-28 for the immersed weight force and III-33 for the wave force into the force balance expression III-37 and solving for the coefficients yields

$$\frac{C_p}{\alpha_1} \tan\phi = \frac{\rho_s \tau_{BF} * R_u^2}{(\rho_s - \rho_w) g m}. \qquad \text{(III-38)}$$

We can let

$$\frac{C_p}{\alpha_1} \tan\phi = K_r \qquad \text{(III-39)}$$

where K_r is a non-dimensional variable. The product of the pivoting relationship, tanϕ, between boulders and ratio of the packing coefficient to the shape factor forms a non-dimensional variable dependent on the distribution of boulder size, shape and the arrangement of boulders within the beach. This variable can be thought of as a complex constant related to boulder stability. This is analogous to the Shields entrainment function, θ_{crit}, as well as the stability coefficient, K_D, in the Hudson Formula (III-1).

Wave tank experiments aimed at finding values for K_D yielded a value of 1.2 for smooth rounded cobbles under wave attack.

Friction and boulder interlocking are factors that oppose entrainment due to lift and drag forces and dynamic pressure forces that develop through wave breaking directly on the beach face and swash run-up. It is possible to write even more complex equations that consider all of the possible force vectors associated wave breaking and swash run-up. However, drag and lift forces depend on depth and velocity both of which change across the beach face during wave run-up, as well as from wave to wave and the dynamic pressure forces depend on breaking wave form. Furthermore, all of these forces act upon boulder surface area that depends on size, shape, and packing arrangements of the boulders within the beach. Therefore, it is also clearly evident that it would be extremely difficult at best to transfer a force vector analysis to a boulder beach exposed to a variable wave and tide climate and also composed of a distribution of boulder sizes and shapes (Fig. III-3). Moreover, it would be entirely impractical if not impossible to measure in the field the projection surface area, pivoting angles and interlocking relationships for all boulders composing a beach. Therefore, friction and interlocking are accounted for with the stability coefficient, K_r, in an analogous manner to the stability coefficient, K_D, of the Hudson Formula, and the wave force is presented as a scalar, III-29, related to wave energy.

The mass, m, of the largest boulder that can be entrained relative to the given wave force is the quantity of interest. Therefore, substitution of III-39 into III-38 and solving for mass, m, yields

$$m = \frac{\rho_s \tau_{BF} * R_u^2}{K_r(\rho_s - \rho_w)g}. \qquad \text{(III-40)}$$

and substitution of τ_{BF}, equation III-27, into III-40 yields

$$M_{R_u} = \frac{\rho_s f_{BF} U_{\max} R_u^{\,3} 2\mathrm{f}}{K_r \left(\frac{\rho_s - \rho_w}{\rho_w} \right) g \tan\theta} \qquad \text{(III-41)}$$

where $M_{R_u} = m$ and refers to the critical threshold mass scaled relative to the run-up elevation. This represents the final form of the wave-competency equation. Equation III-41 can be thought of as a threshold entrainment equation because, as will be shown, it estimates the critical threshold condition of boulder transport on a beach during storms.

One would expect that a slightly larger boulder would have the minimum mass necessary to remain stable. Substitution of the shore break wave height, H_{sb}, for l in equation III-29 yields

$$M_{H_{sb}} = \frac{\rho_s f_{BF} U_{\max} R_u H_{sb}^2 2\mathrm{f}}{K_r \left(\frac{\rho_s - \rho_w}{\rho_w} \right) g \tan\theta}. \qquad \text{(III-42)}$$

Here $M_{H_{sb}}$ represents a boulder mass slightly larger than the predicted threshold entrainment mass, M_{R_u}, because it is scaled to a slightly higher wave energy. Equation III-42 is taken as the minimum mass necessary to maintain stability under the given wave conditions. This expression includes both the wave period and the swash velocity. It is compared with the Hudson formula to illustrate that the mass estimates relate best to static conditions.

FORMULA TESTING AND DISCUSSION

The Data

Field data is used to compare estimates of boulder mass with equation III-41. This data set comes from a field study where boulder transport on a beach was monitored over

a two year period with wave heights and periods recorded by a nearby wave-buoy (Oak, 1985). A range of wave heights and periods are used to further demonstrate the effect of wave period and as a comparison of the stability equation III-42 with the Hudson formula III-1. This analysis compares significant offshore wave height H_S ranging from 1 m to 8 m on 0.5 m intervals and periods of 5, 10, and 15 seconds, respectively. The combination of wave heights and periods covers a range of natural possibilities.

Breaker heights, maximum and average swash velocity, and run-up heights are estimated from the significant deep water wave height, H_s and period, T and the slope of the beach face. Breaker height, H_b, was found using H_s and T with the following empirical expression given by Komar and Gaughan (1973)

$$H_b = 0.39 g^{1/5} (T * H_s^2)^{2/5}. \qquad \text{(III-43)}$$

The stability coefficient K_r was set to one in an attempt to quantify how well the physical variables estimate field data. It is also noted that for smooth round cobbles the stability coefficient K_D of the Hudson formula was found from empirical wave tank data to be equal to a value of 1.2 and one would not expect these stability coefficients to differ greatly.

Kiama Beach Field Data

Kiama Beach is a pocket beach on the South Western coast of Australia. It is 150 m long, 23 m wide with an average slope 0.157 (Oak, 1981). Cliff headlands supply boulder material for the beach that forms a boulder bank throughout the tidal zone with a mean size of 0.256 m (Oak 1981). Oak (1981) monitored the movement of individual boulders from Kiama Beach for a period of two years. The movement of boulders was monitored by establishing a survey grid over the beach and recording the position and size of individual boulders corresponding to each grid point. During the monitoring period Kiama beach was surveyed eleven times following the passing of storms. Wave heights

and periods were recorded from a local offshore wave-buoy. The mass of the largest boulder that had been moved by waves was also recorded. These data were published in Oak (1985) and are arranged here in the first three columns of table 1 in order of increasing wave height of each storm event. The values for the Iribarren number, ξ, for each reported storm event fell within the range appropriate for estimates of run-up height with equation III-5 (Table III-1). Those values are used to compare both equations and the field data of Oak (1985). The value of ρ_S was estimated at 2700 kg/m^3 and the value for stability coefficient, K_D, was taken as 1.2. Values for the stability coefficient, K_D, range from a low value of 1.2 for smooth rounded cobbles to 7 for placed angular stone (table 7-8, SPM 1984). For the Hudson formula larger values of K_D reflect the increased collective strength gained due to interlocking of the placed angular rock.

Table III-1. Oak (1985) data and other variables estimated by the listed equation number.

Oak Data			Supplemental	Analysis			
H_s Buoy (m)	T Buoy (sec)	Largest Boulder (kg)	ξ (III-3) (ND)	H_b (III-43) (m)	$R_{u2\%}$ (III-5) (m)	U_{max} (III-23) (m/s)	Crit. Thr (III-41) (kg)
2.1	10	28	1.35	2.8	1.56	7.91	195
2.2	12	53	1.59	3.12	1.92	8.36	318
2.2	11	93	1.45	3.02	1.76	8.22	262
2.3	11	24	1.42	3.12	1.8	8.36	285
3.2	12	27	1.32	4.21	2.32	9.71	647
3.3	11	39	1.19	4.17	2.16	9.66	567
4.2	14	24	1.34	5.57	3.1	11.17	1523
4.3	14	2191	1.32	5.68	3.13	11.27	1593
5.1	15	898	1.30	6.69	3.65	12.24	2563
5.4	11	1276	0.93	6.19	2.76	11.77	1444
6	12	935	0.96	6.97	3.17	12.49	2137

Comparison of the Critical Threshold Equation with Field Data

The critical threshold equation III-41 adequately approximates (within a factor of 2 to 3) boulder mass at low wave heights of 2 m and gives better estimates (less then a factor of 2) at wave heights above 4.25 m (Fig. III-5). The drop in estimated mass between a wave height of 5.1 m and 5.4 m is due to a respective decrease in wave period from 15 to 11 seconds (Fig. III-5 and Table III-1). This illustrates that increasing wave power also increases the size of boulders that can be transported, confirming the intuitive expectations that lead to the derivation of both equations III-41 and III-42.

The poor correlation between equation III-41 and field data for wave heights less then 4 m is interpreted as due to interlocking and friction between particles dominating the hydraulic forces (Fig. III-5). The friction between particles would be related to size, shape, and packing of the boulders composing Kiama Beach.

Oak (1981) made a plot of wave-buoy data over the beach monitoring period that showed wave heights of 2 m having an approximate 50% exceedance probability, and waves of 4 m a 2% exceedance probability. Storm wave conditions (wave heights > 4 m) are competent to transport the mean boulder size of 0.25 m (Fig. III-5). The D_{90} boulder size for Kiama Beach is 0.7 m (as determined from plots of frequency distributions in Oak 1981). This boulder size is entrained when the deep-water significant wave height exceeds 4.25 m (Fig. III-5).

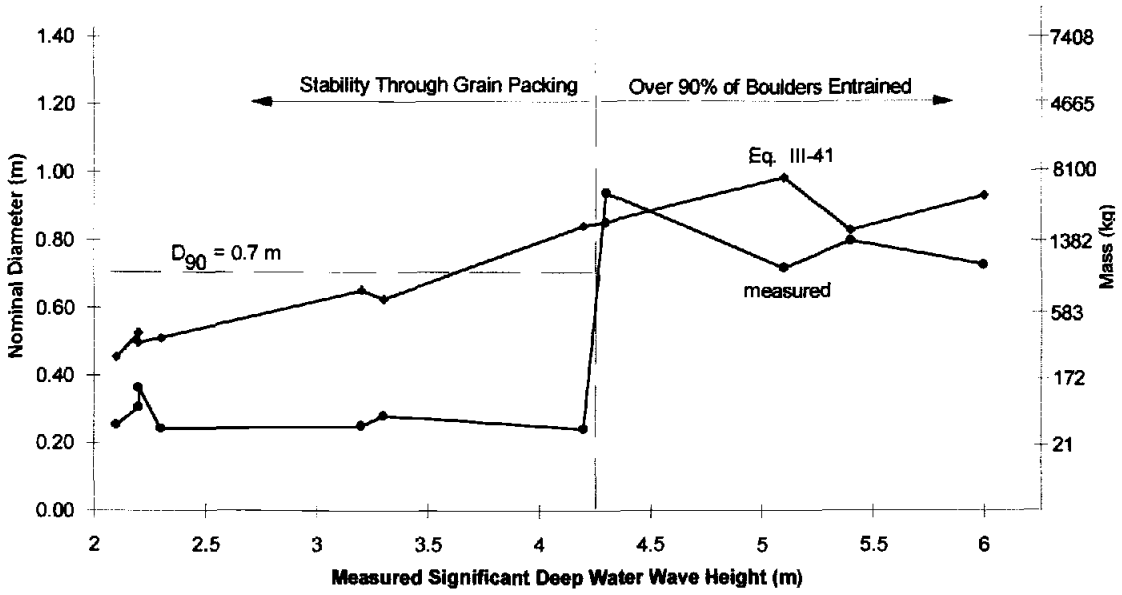

Figure III-5. Comparison between threshold equation III-41 and field data of Oak (1985). The nominal diameter is the diameter of a sphere of equal mass and is included to give a better understanding of the size of the boulders relative to the mass.

It is interpreted that when wave heights exceed 4 m a competent energy level is reached at which point 90 % of the available boulders have the potential to be transported. This size range only becomes mobile during storms where, H_s > ~4 m and it is here where the estimates of threshold mass from equation III-41 more closely match the field data (Fig. III-5). At this high energy regime nearly all boulders composing the beach have the potential for entrainment, and therefore, friction and interlocking between boulders is greatly reduced.

Critical Threshold Versus Minimum Stability

Equation III-41 provides a means for estimating threshold boulder mass for a set of given wave parameters and beach slope. Equation III-42 is similar in that it estimates the minimum stone mass that is stable against movement. The important implication of

having two separate equations is that there are two distinct ranges in boulder size that are estimated both a function of wave period (Fig. III-6). This is very advantageous from a design perspective given that is more desirable to use a size range of quarry material rather than designing for a single size as would be estimated from the Hudson Formula, III-1.

One would expect that the difference between these two ranges should be small. A comparison of estimates for these two equations shows that the difference is indeed small (Fig. III-6). The static range is slightly narrower than the dynamic range, a function of the role wave period and run-up plays in each of the equations. The estimated mass from equation III-41 is dominated by the cube of wave run-up which in turn is a function of wave period. In contrast, the mass estimate from equation III-42 is driven predominately by the square of the breaker height.

Plotting two lines for the Hudson formula in Figure III-8 with K_D values of 1.2 and 7 respectively estimates a tested static range in stone mass relative to a range of wave heights. The value 1.2 is valid for sloping rock structures built with smooth rounded stones and the value of 7 is valid for placed rough angular stones (Table 7-8 SPM, 1984). Together they result in a Hudson stability range dependent on particle interlocking (Fig. III-7). Estimates from the stability equation III-42 for wave periods of 5, 10 and 15 seconds respectively, plot within the stability range of the Hudson formula (Fig. III-7). Results show that the larger is the wave period, the larger is the estimated stable mass.

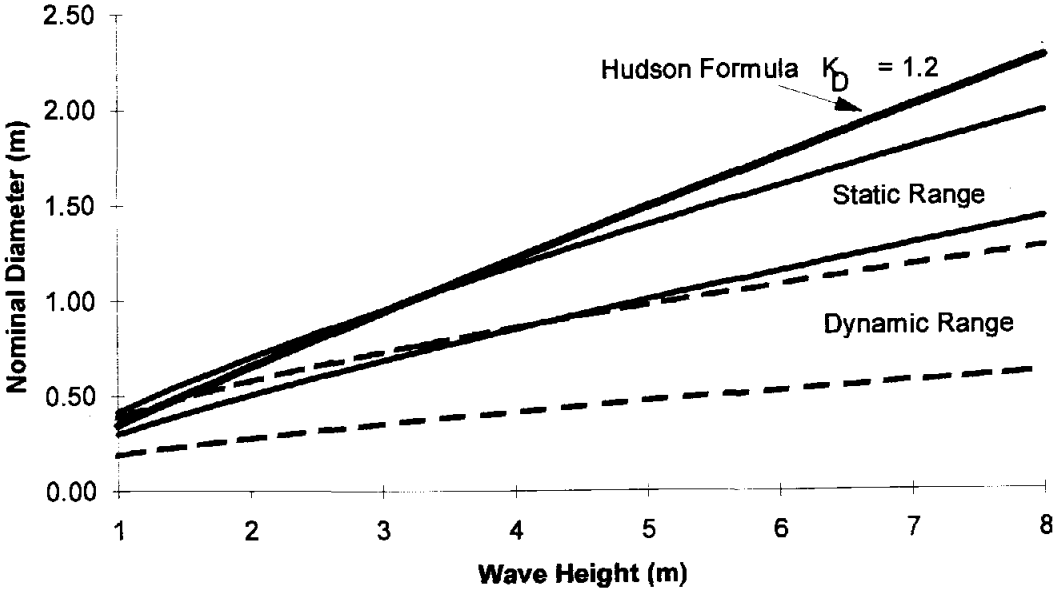

Figure III-6. Comparison of the Hudson formula III-1 with estimates from threshold equation III-41 and the static equation III-42 over a range of wave periods from 5 to 15 seconds.

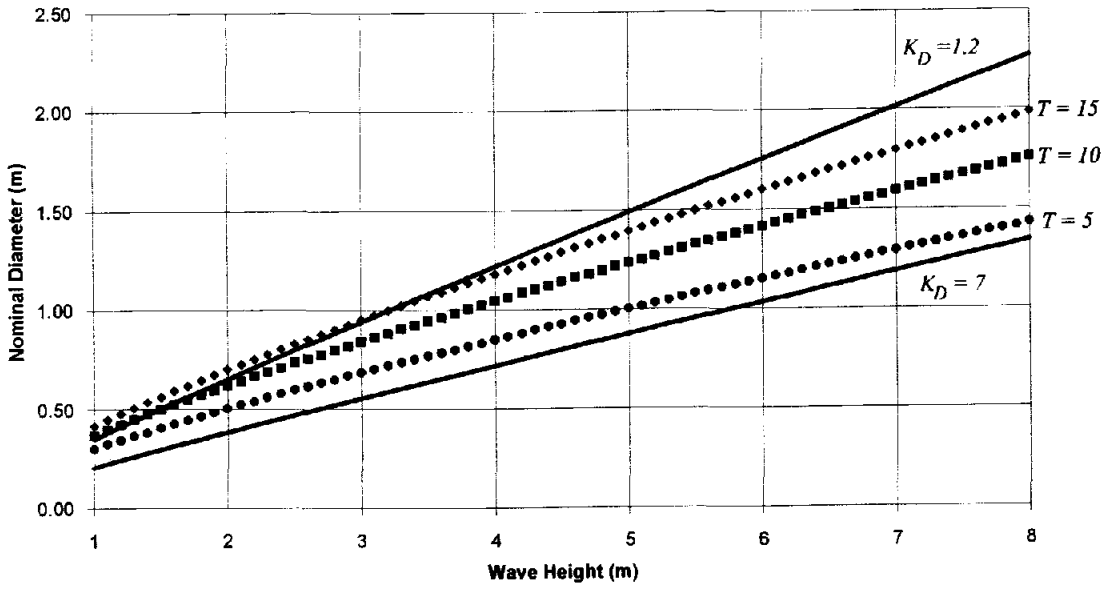

Figure III-7. Comparison of estimates from the Hudson formula III-1 and the stability equation III-42 over a range in wave heights.

Comparing the two equations in this fashion shows that equation III-42 can indeed be considered a static equation, given that estimates lie in or above the static range of the Hudson formula (Fig. III-1). This result is advantageous in that with equation III-42 wave period effects can be addressed when estimating a range of boulder sizes for a static shore-protection structure. The advantage also comes from not having to assume the proper K_r stability coefficient, as compared with the Hudson Formula, III-1, where the proper K_D value depends on estimating angularity of the structure material, mode of placement, morphology (i.e. structure head or trunk) and the expected form of wave breaking.

CONCLUSIONS

The two formulas derived could be useful in the initial evaluation and design of both static and dynamic revetments constructed with unconsolidated quarry stone. These equations offer a significant improvement over the Hudson formula. Equation III-41 was derived to estimate the critical threshold mass, M_{R_u}

$$M_{R_u} = \frac{\rho_s f_{BF} U_{max} R_u^3 2\mathrm{f}}{K_r \left(\frac{\rho_s - \rho_w}{\rho_w} \right) g \tan\theta} \qquad \text{(III-41)}$$

With substitution of H_{sb} for the length scale in the wave force expression, III-29, yields

$$M_{H_{sb}} = \frac{\rho_s f_{BF} U_{max} R_u H_{sb}^2 2\mathrm{f}}{K_r \left(\frac{\rho_s - \rho_w}{\rho_w} \right) g \tan\theta} \qquad \text{(III-42)}$$

where M_{H_b} is the minimum stable mass. Equation III-41 closely approximates the field data of maximum entrained boulder mass (Fig. III-5). Equation III-41 more closely approximates field data at wave heights greater than 4 m (Fig. III-5). This "wave

competency" level of 4.25 m entrains the measured D_{90} grain size fraction (the grain size fraction at which 90 % of the beach material is smaller) for Kiama Beach. Under storm conditions boulder interlocking and friction are second order factors relative to swash velocity, run-up elevation wave height and period. However, empirical testing of III-41 to determine appropriate empirical values for K_r would improve the results.

Increasing wave period will have the effect of transporting larger boulders due to increased wave power. Estimates from equation III-41 when compared with field data (Fig. III-5) and III-42 when compared to a range of wave heights and periods (Figs. III- 6 & 7), support this conclusion. The advantage of equation III-42 over the Hudson formula is that it estimates unit mass in the static range without the need to estimate the value of a stability coefficient. Another advantage is that both III-41 and III-42 estimate a range of rock sizes appropriate for design rather than a single size. Moreover, both equations III-41 and III-42 incorporate the important physical parameters acting on the beach face: breaking wave height, wave period, swash velocity and elevation of the swash run-up, as opposed to relying on an empirical fit with offshore wave conditions. Future testing against field data are necessary to fully evaluate the potential of the derived equations.

CHAPTER 4

PREDICTING THE CREST HEIGHT OF A GRAVEL BEACH

ABSTRACT

The beach crest is a common morphological feature formed by the deposition of sediment carried up-slope by wave swash. The elevation to which waves can pile gravel is a function of: the size and density of the material relative to the hydraulic components of swash velocity, wave frequency and run-up height. Two equations are derived that relate the height of the beach crest to the wave forces and the beach material. The first derivation compares the wave force acting to move a stone up the beach face with a weight force acting to hold the stone in place. The second derivation relates the potential energy per unit area of the beach crest to the total wave energy that lifted and deposited the material above a given sea-level datum. As a test of the derived equations, the actual crest height of one natural gravel beach was accurately estimated by both equations derived. Further research and testing on other natural beaches are needed to verify the equations.

INTRODUCTION

Processes that Form a Beach Crest

The beach crest is a morphological feature that defines the highest elevation above the still water level that waves have piled material. Wave swash can pile gravel and cobble material (i.e., intermediate diameters 0.025 to 0.25 m) several meters above the still water level, given sufficient wave energy. Bagnold (1940) was the first to undertake an experimental approach relating grain size, D and deep-water significant wave height, H_s, to the height of the beach crest

$$h_c = b * H_s \qquad \text{(IV-1)}$$

where h_C is the elevation of the beach crest above the still water level and b is a proportionality coefficient related to the particle size where

$b = 1.68$ for $D = 0.7$ cm,
$b = 1.78$ for $D = 0.3$ cm,
$b = 1.8$ for $D = 0.05$ cm.

Of particular interest is the small range in values for the b proportionality coefficient compared to the relatively large range in particle size indicating that variables other than just wave height may account for more of the expected variance. van der Meer and Pilarczyk (1986) found that wave period had a major effect on crest height while size grading of the material had only a minor one. Bagnold (1940) also observed that the elevation of the beach crest was equal to the height reached by swash surge up the beach face. The elevation that swash surge can reach is referred to as the run-up height. The height to which run-up can reach is a function of energy loss due to friction with the bottom, that lost to sediment transport, internal dissipation of energy due to turbulence and loss of water to percolation. Bagnold (1940) argued that the potential energy carried away by the water that percolates into the beach pebbles results in a situation where the return flow of the backwash can not transport an equal quantity of material just deposited by the previous swash. Bascom (1954) noted that the largest waves were responsible for

the construction of a beach crest given that their swash would completely over-top the existing crest, depositing material as the swash percolated into the beach. This describes the condition under which gravel and coarse sand beaches develop a distinct beach crest above the level of some still-water datum (Fig. IV-1).

Bagnold's (1940) experiments were performed in a glass-walled wave tank where he observed the mode of sediment transport responsible for constructing the beach crest. In all of those experiments, that involved gravel, he reported that the beach crest was formed by material thrown up by the swash of the waves. During intense up-rush of the wave swash the situation exists where swash velocity is much greater than the settling velocity of the gravel composing the beach. Under these conditions stones are not rolled up-slope, but instead are thrown up or transported in a mode of high saltation (Fig. IV-1).

The assumption is made that a beach crest composed of gravel and cobble sized material (i.e., <0.25 m in diameter) develops only during storm wave conditions, where deep-water waves are breaking some distance off-shore, forming a surf zone several breakers wide. Under these conditions the wave attack at the gravel beach could best be described as a bore collapse followed by intense swash up the beach face, resulting in some material being carried to the height of the beach crest of the previous wave or storm event (Fig. IV-1).

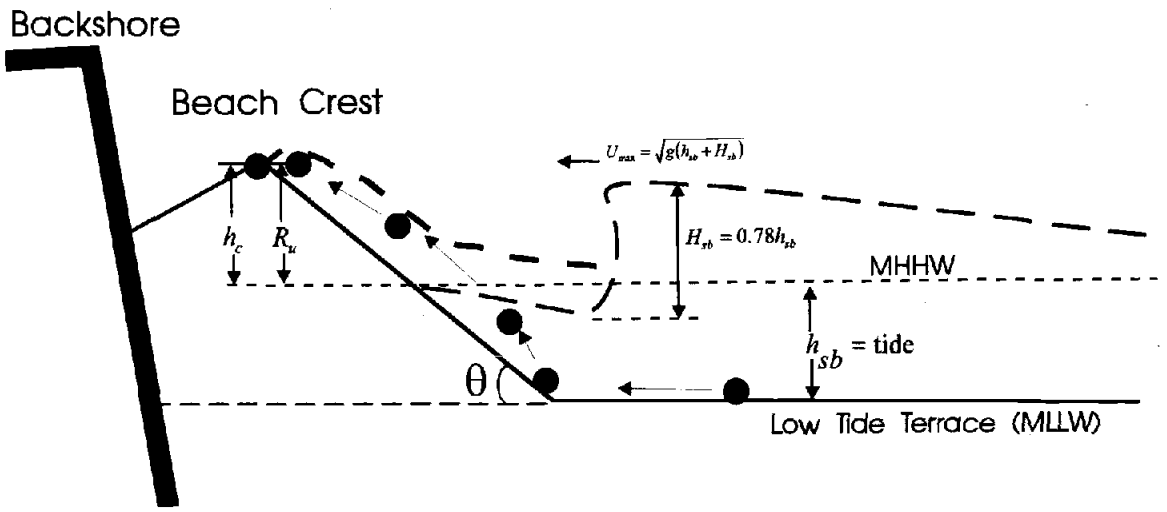

Figure IV-1. Schematic graphic of the process of bore collapse, swash run-up and the suspension of gravel material being thrown up to form the beach crest. The low tide terrace typically corresponds to the mean low tide level given here as mean lower low water (MLLW) for a mixed semi-diurnal tide.

Empirical Relations

Since the initial work by Bagnold (1940) several recent wave tank experiments have provided empirical equations aimed at estimating crest height from wave height, period, storm duration and grain size data (Pilarczyk and der Boer, 1983; van der Meer and Pilarczyk, 1986; van der Meer, 1987; van der Meer and Pilarczyk; 1988; Ahrens, 1990; Ward and Ahrens, 1991; Bradbury and Powell, 1992; van der Meer, 1992; Silvester and Hsu, 1993). The first empirical equation to come from what has become a decade of wave tank work on the dynamics of gravel material under wave attack was the following

$$h_c = D_{90} K \left[C_o H_s g^{-1/2} D_{90}^{-2/3} \sqrt{\cos(\alpha)} \right]^{2/3} \qquad \text{(IV-2)}$$

where D_{90} is the grain size such that 90% of the sediment is smaller, C_o is the deep-water wave celerity, K is a coefficient equal to 0.1 when the argument within [ ] <100 and equal to 0.6 when [ ] >100 and α is the angle of wave approach (Pilarczyk and der Boer, 1983).

Pilarczyk and der Boer (1983) and van der Meer and Pilarczyk (1986) showed that both increasing incident wave height and period resulted in increased berm heights and that the initial beach profile had little effect on the final adjusted profile. More recent work correlated experiment duration, N, representing the number of waves with crest height, h_c, for gravel beaches and coastal engineered breakwaters yielding the following empirical relation

$$h_c = aN^b \frac{H_s}{\sqrt{H_s / L_o}} \qquad \text{(IV-3)}$$

where a and b are correlation coefficients equal to 0.089 and 0.15 respectively (van der Meer, 1992). Silvester and Hsu (1993) present the following equation

$$h_c = 0.302 T \sqrt{H_s} \qquad \text{(IV-4)}$$

using data and empirical relationships developed in van der Meer and Pilarczyk (1988), Ahrens (1990), and Ward and Ahrens (1991).

The above relations (IV-3 and IV-4) show that the height of the beach crest is related to wave height, period, steepness and the number of waves, regardless of the size and density of the beach material. From equation IV-3 we can see that as storm duration increases, or when wave period increases (i.e., $L_0 = 1.56 * T^2$), the height of the beach crest will increase. Intuitively, one can reason that the height of the beach crest must then be related to how wave period affects run-up, swash velocity and the number of swashes that carry sediment to the top of the beach. Equations IV-2, IV-3. and IV-4 are more closely related to run-up on the slopes tested than they are predictive of how high the wave forces can build a beach because mass and density of the beach material are not included.

Maximum wave heights in large wave tanks are on order of 1 m or less and the particle size is on order of 0.01 m. Storm waves generated in the ocean can commonly exceed 6 m annually and particle size typically approaches 1 m for boulder beaches. Consequently, scaling from the wave tank to natural beaches involves uncertainties. Even with these limitations, empirical relationships derived in large wave tanks give insight to the relative importance of the 2-D wave processes active when waves build a beach crest.

It is also intuitive that there would be a maximum crest height related to storm intensity, as well as particle size, density and supply (Orford, J.D., 1977; Forbes, et al., 1995; Orford, J.D., et.al, 1996). Therefore, size and density of the material combined with the morphology of the beach record an amplitude related to the intensity of storm run-up. Scaling the amplitude, h_c, of the beach building process as a function of the wave run-up versus particle size is discussed below.

Estimating Frictional Drag Using Relative Roughness

A minimum requirement for building a beach crest is that particle diameter, D, equals the swash thickness at maximum run-up (Fig.IV-1). If a particle was larger than the swash thickness it would likely not reach the crest due to friction with the beach. The ratio of the elevation of the swash run-up on the beach face, R_u, to the intermediate particle diameter of the largest stone, D_{max}, comprising the beach crest results in a maximum roughness scaling criteria. Therefore, R_u/D_{max}, is a logical ratio for expressing the roughness of the beach face. Scaling relative roughness in this manner is analogous to techniques used to scale flow resistance in rivers. Roughness scaled by the run-up height and maximum particle size of the beach crest can be substituted into equation III-16 yielding

$$C_d = \frac{8}{\left(2.5\ln\left(30\frac{R_u}{D_{max}}\right)\right)^2} \qquad \text{(IV-5)}$$

where C_d refers to form drag associated with particle suspended in a flow.

Sternberg (1972) estimated values of C_d at 0.002 to 0.003 for coarse sand and pebbles (<0.01m diameter material). Voulgaris (et. al., 1994) determined values in the same range for a gravel-bed tidal channel. Wave tank experiments have shown that frictional drag is equal to 0.3 for rough angular rip-rap and closer to 0.05, or less, when dealing with a gravel beach face (Kobushia and Greenwald, 1986; Kobushia et al., 1988; Kobushia and DeSilva, 1989). Data used here for the ratio R_u/D_{max} from a gravel beach on the Oregon coast give an average value of 0.027 for C_d using equation IV-5. This value is close to the reported values from experimental work on frictional drag due to wave swash providing an acceptable way to objectively estimate the frictional drag using easily obtainable physical data. Therefore, equation IV-5 represents a best estimate at this time for C_d.

FORMULA DERIVATIONS

Force Balance Derivation

The main object of this chapter is to derive two equations that relate the height of the beach crest to the hydraulic forces induced by waves and the beach material. The average fluid stress, τ_{BF}, applied to the beach face has been related to the up-slope swash deceleration through the product of maximum and average swash velocity (Chapter III). The assumption made here is that in order to build a beach crest individual stones must either be thrown up to the beach crest or carried in a mode of high saltation by the swash. The wave force, F_{wav}, acting on an individual particle is written in the following manner

$$F_{wav} = \tau_{BF} * D_i^2 \qquad \text{(IV-6)}$$

where D_i^2 is an approximation of the projected surface area of the particle being transported. The minimum critical threshold condition occurs when the wave force, F_{wav}, just equals or exceeds the immersed weight force, F_{wt}

$$F_{wt} = (\rho_s - \rho_w) g D_i^3 \qquad \text{(IV-7)}$$

where ρ_s is the stone density. Equating F_{wav} with F_{wt} describes the minimum critical threshold condition

$$F_{wav} = F_{wt}. \qquad \text{(IV-8)}$$

and substitution yields

$$C_d \rho_w U_{\max} R_u 2 f D_i^2 \cot\theta = (\rho_s - \rho_w) g D_i^3. \qquad \text{(IV-9)}$$

The beach crest height, h_c, can only attain a height equal to the vertical elevation reached by the run-up, R_u, of the wave swash above high tide or some measure of the still water level, h_b (Fig.IV-1). Therefore, by substitution $h_c = R_u$. Solving IV-9 for h_c yields

$$h_c = \frac{(\rho_s - \rho_w) g D_i}{C_d \rho_w U_{\max} 2 f \cot\theta}. \qquad \text{(IV-10)}$$

and with further substitution

$$h_c = \frac{1}{2}\left(\frac{\rho_s - \rho_w}{\rho_w}\right)\left(\frac{g T D_i \tan\theta}{C_d U_{\max}}\right). \qquad \text{(IV-11)}$$

When testing the equation from field data the particle diameter chosen was taken as the mean size, D_{50}. Other studies on gravel transport in rivers have shown that the value for the dimensionless shear stress depends the ratio D_{max}/D_{50}, and is an important scaling parameter when relating critical threshold entrainment to particle size and flow hydraulics (Van Rijn, 1982; Andrews, 1983 and 1984; Carling, 1983; Novak and Nalluri, 1975 and 1984; Komar, 1987a&b; 1988; and 1989). Large values for the ratio indicate the inclusion of a probable erratic that would produce erroneous shear stress values for gravel transport in rivers. The choice of D_{50} size fraction results in a similar scaling ratio within equation IV-11. The use of another size fraction like D_{90} used in equation IV-2 may prove more appropriate given further field testing in the future. However, there is not a good physical reason to chose another value, and therefore, the choice of D_{50} remains somewhat arbitrary.

Equation IV-11 is the first one of interest relating crest height to a balance between the wave forces that are trying to lift a stone above the still water level and the immersed weight force that holds a grain to the beach face. Therefore, equation IV-11 is referred to as a force balance expression relating directly to the physical factors describing the beach material, the wave frequency, swash velocity and associated drag as a function of the relative roughness of the beach face.

Potential Energy Derivation

The second equation used to predict the height of the beach crest is derived by first defining the potential energy of a mass of beach material elevated above some sea level datum. The potential energy, *PE*, of a mass of material composing the beach crest should closely equal the total energy, E, of the waves that put the material there minus friction

$$PE = E - friction. \qquad \text{(IV-12)}$$

The expression for wave energy is given by linear wave theory as

$$E = 1/8 g \rho_w H_{sb}^2 \ . \qquad \text{(IV-13)}$$

The potential energy, *PE*, can be written in the following manner

$$PE = mgh_c \qquad \text{(IV-14)}$$

where m is the mass per unit area of beach crest. The assumption is made that the grains are put into suspension by the swash and are thrown up the beach face forming the crest. Those grains that are not put into suspension would subsequently not reach the crest due to friction. Substitution of equations IV-13 and IV-14 into equation IV-12 neglecting friction and solving for beach crest height, h_c, results in the following expression

$$h_c = \frac{\rho_w H_{sb}^2}{8m}. \qquad \text{(IV-15)}$$

Both equations IV-11 and IV-15 incorporate tide elevation into the derivation. The tide enters equation IV-11 through the estimation of the maximum swash velocity, U_{max}, with the appropriate expression for the shallow water wave celerity equation at the shore break

$$U_{\max} = \sqrt{g(h_{sb} + H_{sb})} \qquad \text{(IV-16)}$$

where h_{sb} is the tidal elevation above the mean lower low tide (Fig. IV-1). Gravel beaches typically are fronted by a low sloping sand beach or wave cut bedrock terrace where the slope inflection corresponds with mean low water (Nicholls, 1988 and 1990).

This allows the tide elevation above mean low water to be used as a close approximation of water depth (Fig. IV-2). The tide enters equation IV-15 through the following expression for the breaking condition.

$$H_{sb} = 0.78 h_{sb} \qquad \text{(IV-17)}$$

Komar (1976).

FORMULA TESTING AND DISCUSSION

Model Test

In order to estimate the height of the beach crest, both the empirical equations IV-2, IV-3, IV-4 and those derived here IV-11 and IV-15 require the following data: wave height, H_s, period, T, the average highest high tide, h_{sb}, some measure of grain size, D_i, beach slope, and the average mass per area of the beach crest (Fig. IV-2). To obtain these required data a beach was surveyed and sediment samples were collected from the beach crest (Fig. IV-2). An analysis of wave data covering the time period over which the beach morphology was observed to have developed provide the necessary wave and tide statistics. A discussion follows of how these data were measured in the case of the beach and determined in the case of the storm-wave conditions.

Physical Description of Short Beach

A coarse grained beach (i.e. boulders to gravel) located on the Oregon Coast and known locally as Short Beach was chosen to test the equations (Fig. IV-3). Short Beach is a small pocket beach bounded on the north by Cape Mears, and the headland of Three Arch Rocks National Wildlife Refuge (Fig. IV-3). The beach morphology was surveyed on 4-18-96 with a total station. Twelve backshore headstakes were established (A-L Fig. 4 top). Their elevation above mean lower low water (MLLW) was determined from the

reported elevation survey monument 15-5A established in 1968 by the Oregon State Highway Department.

The sediment supply for Short Beach comes from a landslide that dumps material from a broken basalt flow on to the beach (Fig. IV-4 top). The landslide material ranges in size from boulders several meters in diameter to angular gravel and sand. A clear southward gradation from boulders to cobbles occurs across the front of the landslide (Fig. IV-4 bottom). A gravel beach begins at headstake G extending to A (Fig. IV-4 bottom). The grain size plotted for the gravel beach (G to A) are for the maximum grains and the mean size is plotted for landslide area (H through L).

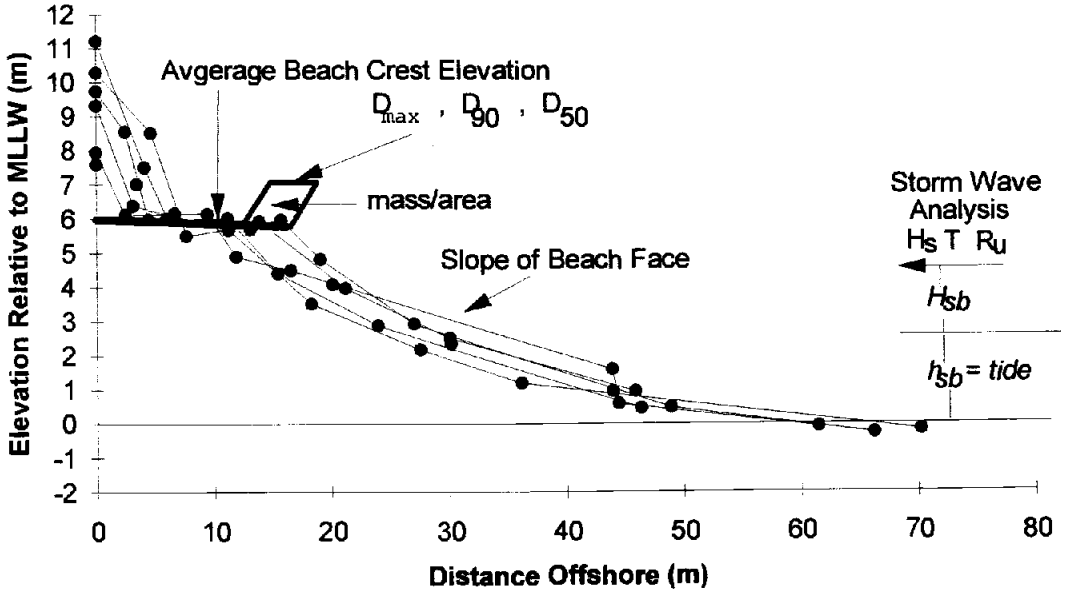

Figure IV-2. Graphic showing the survey data points of a gravel beach and the related information needed to test and compare equations IV-2, IV-3, IV-4, IV-11 and equation IV-15. Note that the base of the gravel beach face closely approximates mean lower low water level.

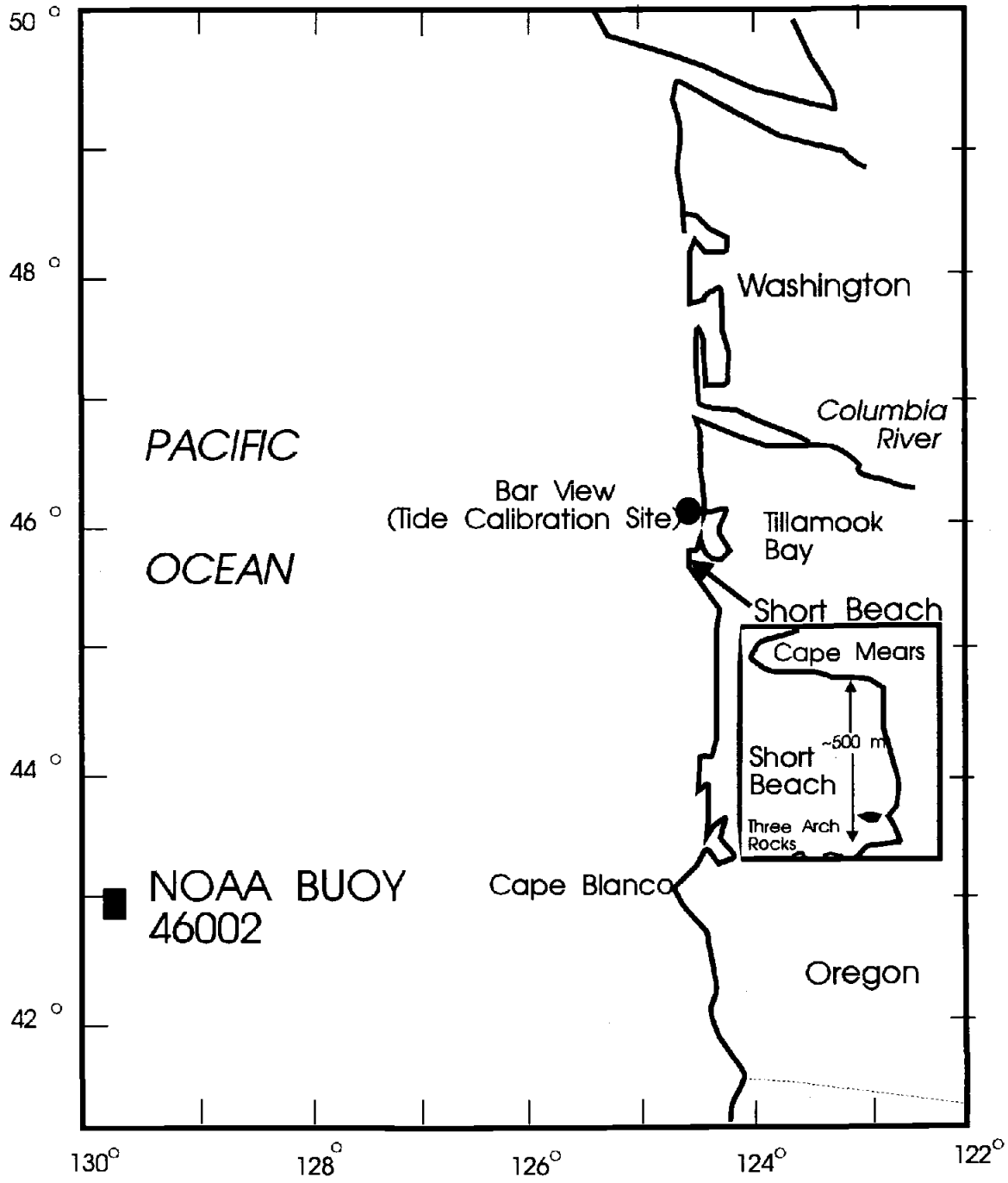

Figure IV-3. Location map showing Short Beach and the NOAA buoy and tide calibration site.

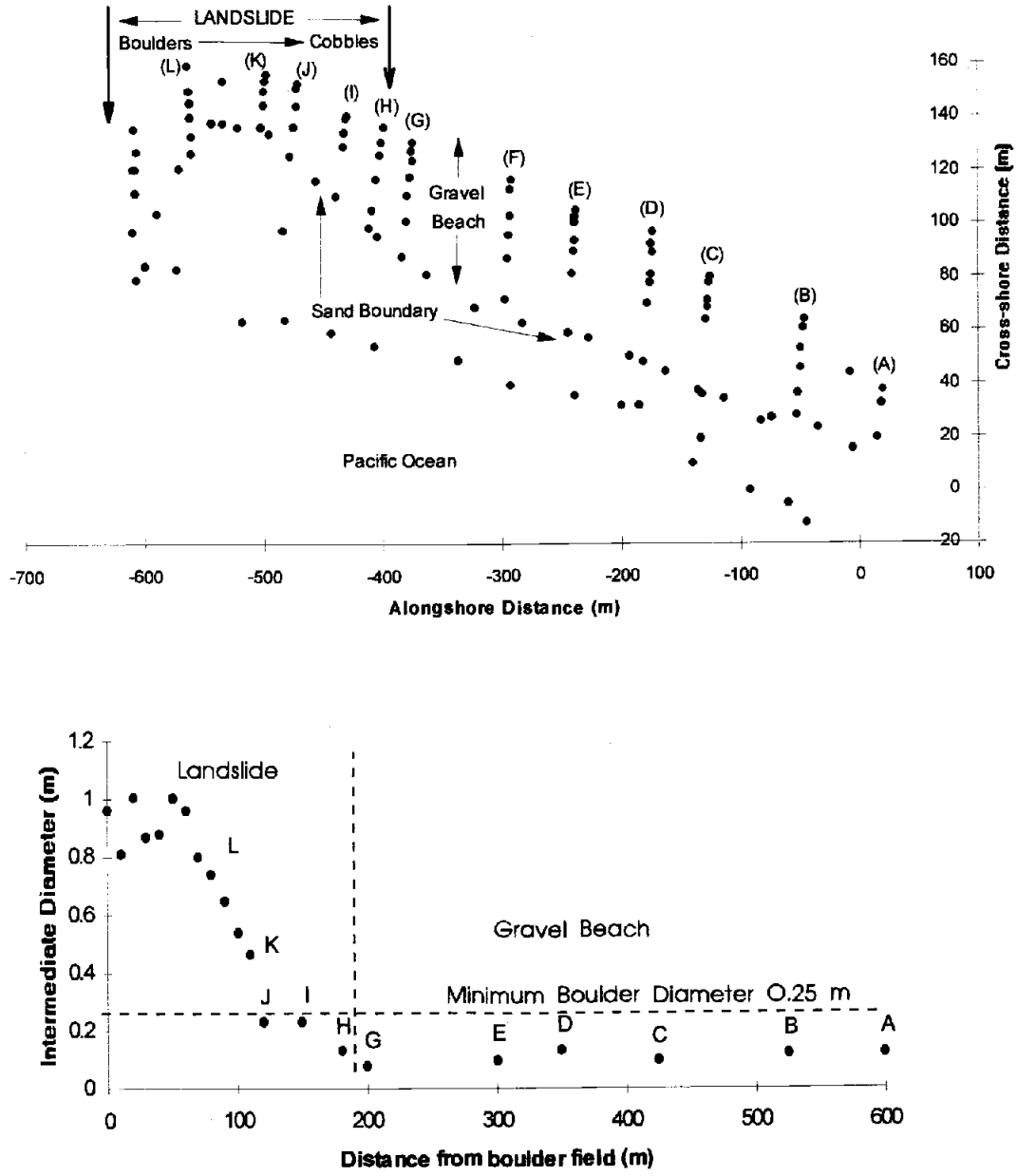

Figure IV-4. Horizontal coordinates for the survey data of Short Beach (Top). Particle size gradation as a function of distance from the landslide area (Bottom).

A total of 319 boulders composing the beach between the northern border and headstake K were measured with a meter stick. A 1 m^2 grid was used to delineate an area of the mid-beach face fronting headstakes (H, I, & J) from which the three orthogonal

axes of the cobbles and boulders falling within the grid were measured. A 0.25 m^2 grid was used to collect samples from the beach crest fronting headstakes (A-G). Each 0.25 m^2 grid was sampled to a depth equal to the size of the largest rock that fell within the grid. The mass of each sample from the 0.25 m^2 grid was measured with a spring scale. Summary statistics of all the grain size data from the beach crest appears in table IV-1.

Table IV-1. Particle diameters, sample mass and surveyed crest height corresponding to the headstake ID as shown in figure IV-4 top.

ID	D_{max} b-axis (cm)	D_{90} b-axis (cm)	D_{50} b-axis (cm)	Sample mass (kg/m^2)	Crest height (m)
A	12	10.2	6.8	100	5.89
B	12	7.5	5.0	96	5.67
C	10	7.5	4.85	98	6.14
D	13.4	11.8	8.37	114.8	5.96
E	10.3	9.4	5.5	63.2	6.03
F	8.3	7	4.92	48	5.92
G	12.5	8.8	6.09	80	6.15
AVG	11.21	8.9	5.93	84.4	5.97

The main supply of the large boulders occurs in the area of the landslide and it is this area that extends furthest seaward into the surf zone at high tide (Fig. IV-4 top). An extensive gravel beach begins at headstake G and extends for 500 m to headstake A (Fig . IV-4). The gravel beach section (headstakes A-G) was characterized by a distinct crest extending 10 to 15 m seaward from the backshore location of the headstakes (Fig. IV-5). The beach crest was built by storm wave action between 1-1-95 and 4-18-96 (personal

observation) to an average elevation of 5.9 m (Table 1 and Fig. IV-5). The beach crest was built to an approximate elevation of 6 m above MLLW (Fig. IV-5). A distinct boundary between the steep faced gravel beach and the sandy low tide terrace was surveyed on 4/18/96 at an average elevation of 1 m above MLLW (Fig. IV-5). This boundary advances shoreward in response to swell waves and seaward during storms. The average slope of the beach face was 0.15 (m/m).

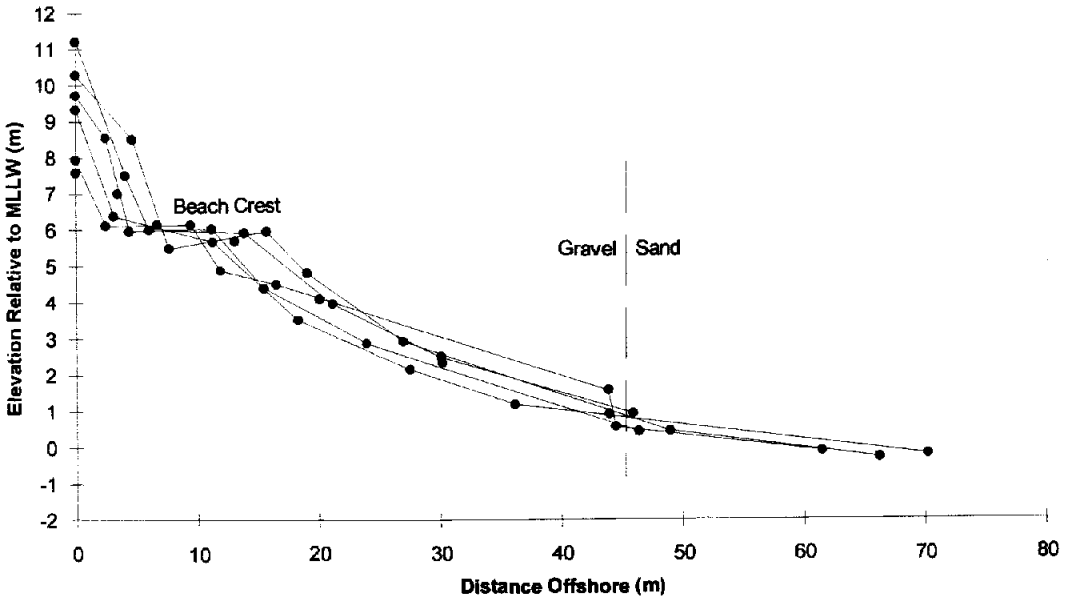

Figure IV-5. Shore normal survey transect lines and data points extending seaward from the headstakes (B-G) are shown. The headstake locations are show in figure IV-4 top.

Wave and Tide Data Analysis

An analysis of wave and tide data revealed five major storms most likely responsible for building the beach crest surveyed on 4/18/96 (Fig. IV-5). The wave data comes from NOAA buoy # 46002 (Fig. IV-3). It was chosen over several buoys located closer to Short Beach given that it had a complete wave record over the period of interest from (1-1-95) to (4-18-96). A recent study (Tillotson, 1997) demonstrated that the deep-

water wave climate is essentially uniform along the Pacific Northwest coastline. Therefore, choosing the more complete record was more important than choosing the closest wave recorder. The wave data is composed of hourly averages of significant wave height and dominant wave period. Corresponding hourly tide estimates were produced with a software package that bases predictions on NOAA data (Nautical Software, 1996). Corrected time and value adjustments were complete for Tillamook Bay, Barview, an exposed ocean site located approximately 10 kilometers north of Short Beach (Fig. IV-3).

A time-series plot of deep-water wave power was calculated for each hourly increment of the wave record (Fig. IV-7 top). Deep-water wave power, $P_l = E*C_g$, represents the available force that can do work on the beach. Five relatively significant storms are apparent from the plot of wave power (Fig. IV-6 top). The difference between winter storms and summer swell is also clearly evident (Fig. IV-6 top).
Deep-water wave power is the first component of interest. However, the elevation of wave run-up on the beach coupled with the tide level at the time of the storm is also a major factor. The elevation of the beach crest is determined by how high the run-up of the wave swash can pile material. A time-series of wave run-up plus tide (Fig. IV-6 middle) versus the mean height of the beach crest reveals which storms with significant wave power actually were able to overtop the beach crest (Fig.IV-6 middle). It is clear that some wave events that were not of significant wave power were able to reach the top of the beach crest given that they occurred during monthly tidal maximum (wave events during Sept. through Nov. 1995).

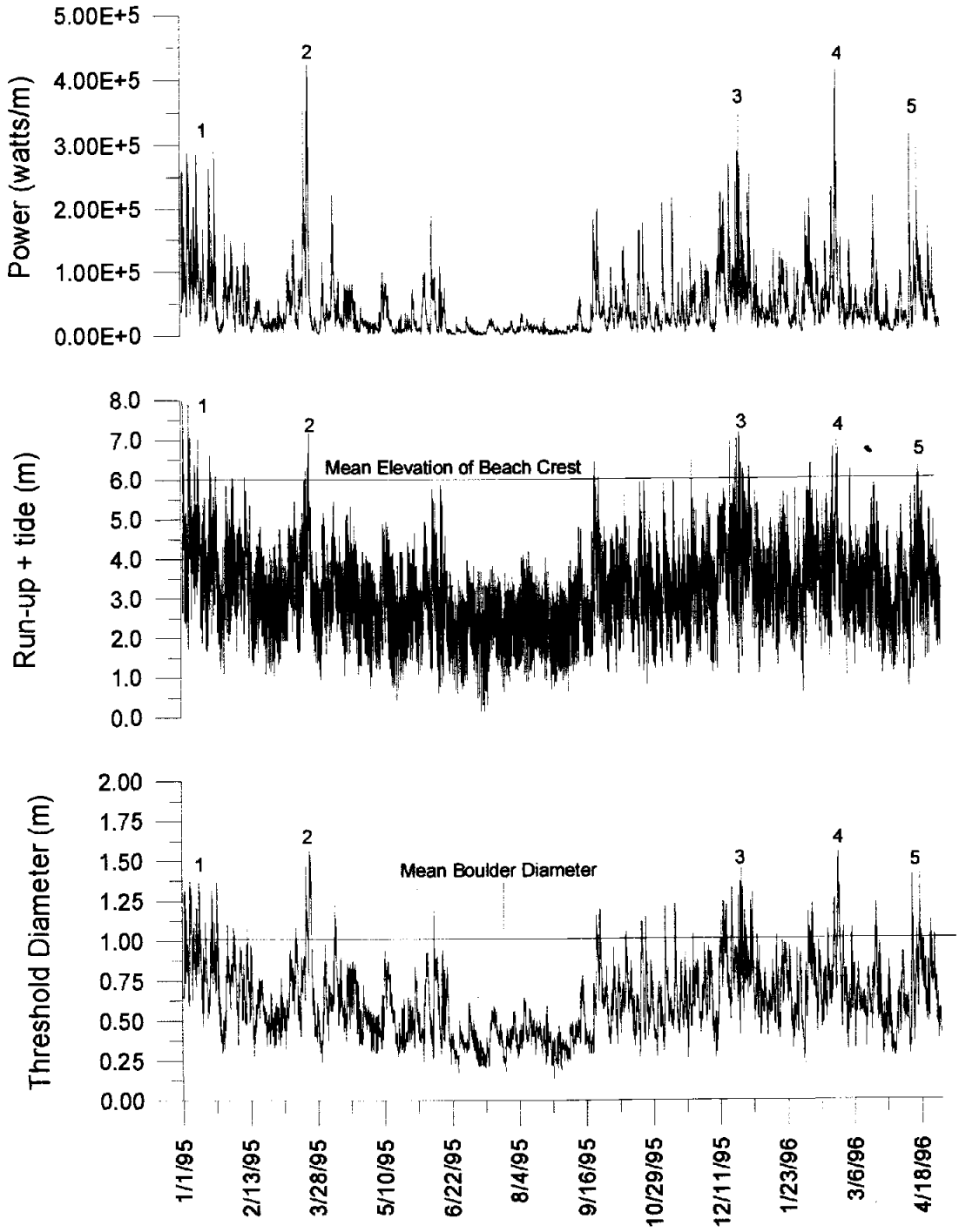

Figure IV-6. A time-series plot of deep-water wave power prior to the survey date of 4/18/96 (top). The time-series of estimated run-up height plus the tide level is plotted versus the surveyed beach crest elevation (middle). A time-series plot of estimated threshold diameter is shown on the bottom. Five storm-wave events are identified.

Further evaluation of which storms are responsible for building the surveyed beach crest required a time-series plot of the predicted critical threshold mass calculated utilizing equation (III-41) derived in chapter 3. The nominal particle diameter of a sphere of the same mass was then determined and plotted (Fig. IV-6 bottom). The time-series plot of the critical threshold diameter in comparison with the one meter boulder diameter indicates that each identified storm satisfied the requirement that wave force active during these storms be greater than the critical threshold conditions for gravel.

Field Data Results

Estimates of beach crest height, for Short Beach, can be made given the values taken from the storm analysis (Table 2) the measured slope of the beach face and mean grain size of the material forming the beach crest (Fig. IV-7). It was concluded that one, or all, of the identified storms deposited the sampled sediment found at the measured beach crest for each transect (A-G)). Equation IV-3 an estimate of the number of waves, *N*. This was done by summing the minutes where run-up equaled or exceeded the surveyed elevation of the beach crest for each of the five identified storm events shown in the middle panel of figure IV-6. The significant number of waves was then calculated by dividing the total minutes for each storm that run-up equaled or exceeded the beach crest by the average wave period for the duration. Stone density, ρ_s, was determined by measuring the mass of several stones and the volume of water they displaced, resulting in a value of 2,772 kg/m^3. The density of sea water, ρ_w, was taken as 1,025 kg/m^3.

The estimates of crest elevation utilizing these data were compared between equations IV-2, IV-3, IV-4 and those derived here equations IV-11 and IV-15 and the surveyed beach crest elevation (Fig. IV-8). The angle of wave approach is essentially zero due to wave refraction (e.g. $\sqrt{\cos\alpha} = 1$), and therefore, the K is a coefficient equal to 0.6 given that [ ] >100 for equation IV-2. The tide elevation of 2.5 m was added to the

results from equations IV-2, IV-3 and IV-4 given that these equations predict crest height above the still water level in wave tanks.

Table IV-2. Statistical results from storm analysis.

#	Storm Date	Mean Wave Ht (m)	Peak Period T (sec.)	Tide max (m)	Dur. Sig Run-up (min.)	Sig. # of Wav (Dur/avgT)
1	Jan. 95	5.3	15.8	2.7	35	150
2	March 95	6.7	14.7	2.3	42	180
3	Dec. 95	6.3	14.3	2.3	53	220
4	Feb. 96	5.9	13.4	2.4	38	160
5	April 96	5.3	14	2.8	48	200
	AVERAGE	5.9	14.4	2.5	43	180

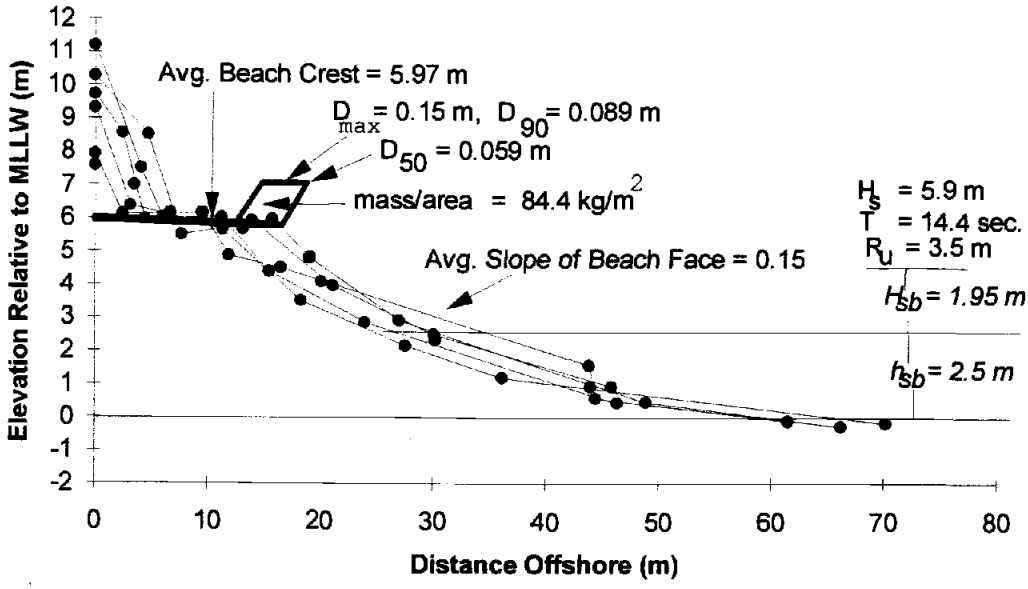

Figure IV-7. Survey profile data and the necessary variables to test the equations.

The estimated height of the beach crest above MLLW from equation IV-11 is 6.1 m and the predicted crest height from equation IV-15 is 5.8 m. The difference between these estimates and the actual average measured crest height (6.0 m) is close to the maximum particle diameter (0.22 m) found on the beach crest (table 1 D). The two equations derived here closely estimate the surveyed elevation of the beach crest at Short Beach, Oregon (Fig. IV-8).

The estimate of U_{max} in equation IV-11 with equation IV-11 simply adds wave height, H_{sb}, to the water depth rather than wave amplitude (e.g. $1/2H_{sb}$). This results in an increased water depth for the estimate of U_{max} approximately 1 m greater than adding just the wave amplitude. This in part compensates for not directly including the effects of wave set-up, given that it could elevate the water column during storms on the order of a meter. Set-up is not accounted for in equation IV-15. One could argue that it should be included, making the prediction from IV-15, 6.8 m rather than 5.8 m. However, including set-up in equation IV-15 would not improve the prediction (Fig. 8).

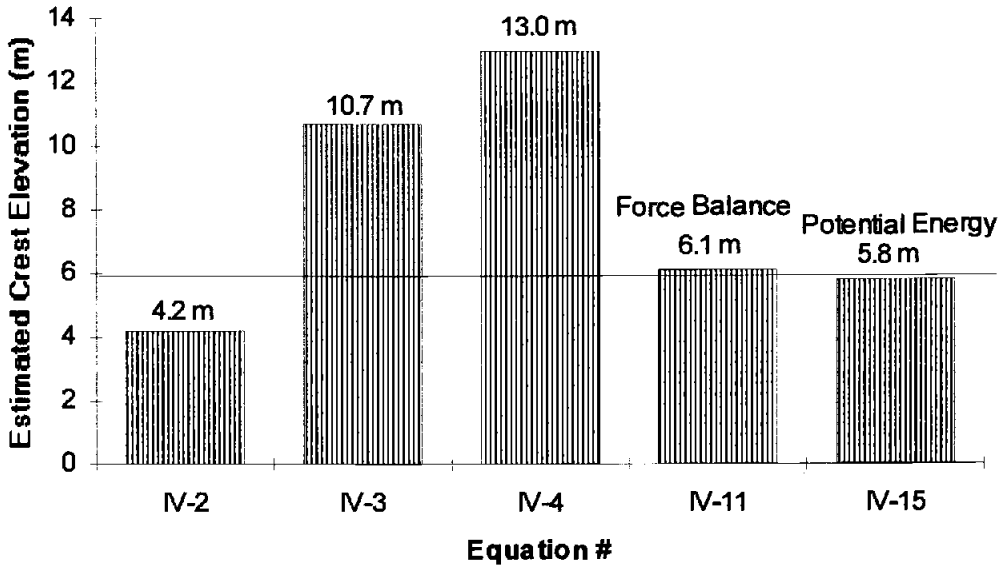

Figure IV-8. Comparison of the estimates from equations IV-2, IV-3, IV-4, IV-11, IV-15 with the surveyed crest height of 5.9 m.

CONCLUSIONS

Two equations that relate the height of the beach crest to the wave forcing and the beach material were derived. Both derivations rely on the assumption that gravel is thrown up to form a beach crest or moved in a mode of high saltation during wave swash up the beach slope. The estimate of crest height from equation IV-11 is a force balance expression relating directly to the physical factors describing the beach material, the swash velocity, frequency and associated drag as a function of the relative roughness of the beach face

$$h_c = \frac{1}{2}\left(\frac{\rho_s - \rho_w}{\rho_w}\right)\left(\frac{gTD_i \tan\theta}{C_d U_{\max}}\right). \qquad \text{(IV-11)}$$

The derivation of the second equation IV-15 relates the potential energy of a mass of beach material elevated above some sea level datum to the wave energy that deposited it

$$h_c = \frac{\rho_w H_{sb}^2}{8m}. \qquad \text{(IV-15)}$$

Both equations IV-11 and IV-15 accurately estimated the crest height of one natural gravel beach (Fig. IV-8). However, further field testing of these equations is required to fully except their validity in predicting the elevation of a gravel beach crest.

GENERAL CONCLUSIONS

The general theme is that the size of the largest stone composing a coarse grained deposit reflects the magnitude of the hydraulic event that last transported it. This concept has been referred to in past riverine work as flow competence. It is based on the intuitive notion that threshold shear stress can be inferred from the size of the largest particles transported by open channel flow. This idea is applied here to the beach environment. To do this the quantitative techniques employed in the riverine environment are modified to apply to wave swash on boulder and gravel beaches. Therefore, the term wave competence is used here to refer to the ability of waves to entrain boulders and gravel particles composing a beach in a manner similar to the concept of flow competence in rivers.

There were three main objectives for this dissertation.

- The first objective was to critically examine accepted flow competence techniques as a method for assessing the mobility potential of bank-full discharge for steep-gradient gravel- and boulder-bed rivers.
- The second objective was to derive two wave competence equations for boulders on a beach: one to estimate critical threshold mass and another to estimate minimum stable mass.
- The third objective was to derive two more equations that relate the elevation of gravel beach crest, above a common water level datum, to the wave forcing and the beach material.

Conclusions Applicable to Objective One

A reformatted Shields relation, $\tau_{crit} = 0.045(\rho_s - \rho_w)gD_{50}^{0.6}D_{max}^{0.4}$, is used to estimate the shear stress required to remobilize the maximum-size particles from 33 high-gradient river reaches having bed material ranging in size from gravel to boulders. The analysis

uses a mobility ratio, expressed as the shear stress during bank-full conditions, $\tau_b = 1/8\, f_r \rho_w U^2$, over the reformatted Shields entrainment stress calculated from the size of the bed material. The mobility ratio, τ_b / τ_{crit}, for bank-full discharge is much less then unity for most of the 33 sites examined. As the bed material becomes coarser the ability of the bank-full shear stress to reach critical threshold entrainment levels decreases (Fig. II-4). Furthermore, nearly an order of magnitude increase in shear stress would be necessary to entrain boulder size substratum (Fig. II-4). Increasing discharge above bank-full conditions would for the most part only cause inundation as the flood waters over top the bank. This would not theoretically cause a sufficient increase in shear stress.

The reformatted Shields relation does not take into account collisions between particles. This process would transfer momentum more efficiently to the bed than a clear flow, and thereby, entrain larger grains than expected from only the fluid shear stress. Therefore, it is concluded that the extension of the reformatted Shields equation to flood deposits and boulder-bed rivers in order to estimate past hydraulic conditions or to determine flushing flows for regulated rivers could result in significant error.

Conclusions Applicable to Objective Two

The two formulas derived could be useful in the initial evaluation and design of both static and dynamic revetments constructed with unconsolidated quarry stone. These equations offer a significant improvement over the Hudson formula. Equation III-41 was derived to estimate the critical threshold mass, M_{R_u}

$$M_{R_u} = \frac{\rho_s f_{BF} U_{\max} R_u^{\,3} 2\mathrm{f}}{K_r \left(\frac{\rho_s - \rho_w}{\rho_w} \right) g \tan\theta} \qquad \text{(III-41)}$$

With substitution of H_{sb} in the derivation, an expression results having the form

$$M_{H_{sb}} = \frac{\rho_s f_{BF} U_{max} R_u H_{sb}^2 2\mathrm{f}}{K_r \left(\frac{\rho_s - \rho_w}{\rho_w} \right) g \tan\theta} \qquad \text{(III-42)}$$

where M_{H_b} is the minimum stable mass. Equation III-41 closely approximates the field data of maximum entrained boulder mass (Fig. III-5). Equation III-41 more closely approximates field data at wave heights greater than 4 m (Fig. III-5). This "wave competency" level of 4.25 m entrains the measured D_{90} grain size fraction (the grain size fraction at which 90 % of the beach material is smaller) for Kiama Beach. Under storm conditions boulder interlocking and friction are second order factors relative to swash velocity, run-up elevation and wave period. However, empirical testing of III-41 to determine appropriate empirical values for K_r would improve the results.

Increasing wave period will have the effect of transporting larger boulders due to increased wave power. Estimates from equation III-41 when compared with field data (Fig. III-5) and III-42 when compared to a range of wave heights and periods (Figs. III-6 & 7), support this conclusion. The advantage of equation III-42 over the Hudson formula is that it estimates unit mass in the static range without the need to estimate the value of the stability coefficient, K_D. Also of advantage is that both III-41 and III-42 estimate a range of rock sizes appropriate for design rather than a single size. Moreover, both equations III-41 and III-42 incorporate the important physical parameters acting on the beach face: breaking wave height, wave period, swash velocity and elevation of the swash run-up, as opposed to relying on an empirical fit with offshore wave conditions. Future testing against field data are necessary to fully evaluate the potential of the derived equations.

Conclusions Applicable to Objective Three

Two equations that relate the height of the beach crest to the wave forcing and the beach material were derived. Both derivations rely on the assumption that gravel is thrown up to form a beach crest or moved in a mode of high saltation during wave swash up the beach slope. The estimate of crest height from equation IV-11 is a force balance expression relating directly to the physical factors describing the beach material, the swash velocity, frequency and associated drag as a function of the relative roughness of the beach face

$$h_c = \frac{1}{2}\left(\frac{\rho_s - \rho_w}{\rho_w}\right)\left(\frac{gTD_i \tan\theta}{C_d U_{\max}}\right). \qquad \text{(IV-11)}$$

The derivation of the second equation IV-15 relates the potential energy of a mass of beach material elevated above some sea level datum to the wave energy that deposited it

$$h_c = \frac{\rho_w H_{sb}^2}{8m}. \qquad \text{(IV-15)}$$

Both equations IV-11 and IV-15 accurately estimated the crest height of one natural gravel beach (Fig. IV-8). However, further field testing of these equations is required to fully except their validity in predicting the elevation of a gravel beach crest.

BIBLIOGRAPHY

Ahrens, J., and McCartney, B.L., 1975. Wave period effect on the stability of riprap. *Proc. Civil Engr. in the Oceans/III*, American Society of Civil Engineers pp. 1019-1034.

Ahrens, J. P., 1981. Irregular wave runup on smooth slope. *Tech. Aid No. 81-17, Coastal Engineering Research Center,* Waterways Experiment Station, Vicksburg, Miss.

Ahrens, J. P., 1990. Dynamics revetments. *Proc. 22nd Inter. Conf. Coastal Eng.*, ASCE 2: pp. 1837-50.

Allen, J.R., 1970. *Physical processes of sedimentation.* American Elsevier Pub., New York. 248 p.

Allsop, N.W.H., Franco, L., and Hawkes, P.J. 1985. Wave run-up on steep slopes - a literature review. *Report NO. SR 1, Hydraulic Research,* Wallingford U.K.

Andrews, E.D., 1983. Entrainment of gravel from naturally sorted riverbed material. *Geological Society of American Bulletin.* v. 94, pp.1225-1231.

Andrews, E.D., 1984. Bed-material entrainment and hydraulic geometry of gravel-bed rivers in Colorado. *Geological Society of American Bulletin.* v. 95, pp. 371-378.

Ashworth, P.J. and Ferguson, R.I., 1989. Size-Selective entrainment of bedload in gravel bed streams: *Water Resources Research.*, v. 25, No. 4, pp. 627-634.

Bagnold, R.A., 1940. Beach formation by waves some model experiments in a wave tank. *Jour. Inst. C.E.*, 15, Paper No. 5237, pp. 27-52.

Bagnold, R.A., 1966. An approach to the sediment transport problem from general physics: *U.S. Geol. Survey Prof. Paper:* 422-I.

Baker, V.R., and Ritter, D.F., 1975. Competence of rivers to transport coarse bedload material: *Geol. Soc. America Bull.*, v. 86, pp. 975-978.

Bascom, W.H., 1954. Characteristics of natural beaches. *Proc14th Conf. Coastal Eng.*, pp. 163-180.

Battjes, A.J., 1974.(a) Surf Similarity. *Proc. 14th Conf. Coastal Eng.*, ASCE, pp. 466-480.

Battjes, A.J., 1974. (b) Computation of set-up, longshore currents, run-up and overtopping on steep-slopes due to wind-generated waves. *Report 74-2. Committee on Hydrualics, Dept. of Civil Engineering.* Delft Univ. of Technology, Delft, the Netherlands.

Bradbury, A.P., and Powell, K.A., 1992. The short term response of shingle spits to storm wave action. *Coastal Engineering*, v.16, pp. 2695-2707

Bradely, W.C., and Mears, A.I., 1980. Calculations of flows needed to transport coarse fraction of Boulder Creek alluvium at Boulder, Colorado: *Geol. Soc. America Bull.*, v. 86, pp. 1057-1090.

Bridge, J.S., and Bennett, S.J., 1992. A model for the entrainment and transport of sediment grains of mixed sizes, shapes, and densities: *Water Resources. Research*, v. 28, pp. 337-363.

Bruun, P., and Gunbak, A.R., 1977. Stability of sloping structures in relation to $\xi = \tan\alpha/\sqrt{H/L_o}$ risk criteria in design. *Coastal Engineering* 1, pp. 287-322.

Carling, P.A., 1983. Bedload transport in two gravel-bedded streams: *Earth Surface Processes and Landforms.* v. 14, pp. 27-39.

Carling, P.A., Kelsey, A., and Glaister, M.S., 1992. Effect of bed roughness, particle shape and orientation on initial motion criteria: In *Gravel-bed Rivers:* Hey,R.D., Bathurst, J.C. and Thorne,C.R., pp. 23-39.

Chow, V.T., 1959. *Open Channel Hydraulics.* McGraw Hill, New York, 640 p.

Costa, J.E., 1983. Paleohydraulic reconstruction of flash-flood peaks from boulder deposits in the Colorado Front Range: *Geol. Soc. America Bull.*, v. 94, pp. 986-1004.

Dalrymple, R.A., 1992. Prediction of storm/normal beach profiles. *Jour. of Waterway Port, Coast, and Ocean Eng.* v.118, pp.193-200.

Drake, T.G., Shreve, R.L., Dietrich, W.E., Whiting, P.J. and Leopold, L.B., 1988. Bedload transport of fine gravel observed by motion-picture photography: *J. Fluid Mech.*, v. 192, pp. 193-217.

Forbes, D.L., Orford, J.D., Carter, R.W.G., Shaw, J., and Jennings, S.C., 1995. Morphodynamic evolution, self-organisation, and instability of coarse-clastic barriers on paraglacial coasts. *Marine Geology* 126 pp. 63-85.

Gilbert, G.K., and Murphy, E.C., 1914. The transport of debris by running water: *U.S. Geol. Survey Prof. Paper* 86, 236 p.

Grass, A.J., 1970. Initial instability of fine bed sand: *Jour. Hydraulics Div., Amer. Soc. Civil Engrs.*, 96: HY3, pp. 619-632.

Hammond, F.D.C., Heathershaw, A.D., and Langhorne, D.N., 1984. A comparison between threshold criterion and the movement of loosely packed gravel in a tidal channel: *Sedimentology*, v. 31, pp. 51-62.

Hassan, M.A., and Reid, I., 1990. The influence of microform bed roughness elements on flow and sediment transport in gravel bed rivers: *Earth Surface Processes and Landforms*, v. 15, pp. 739-750.

Helley, E.J., 1969. Field measurement of the initiation of large particle motion in Blue Creek near Klamath, California: *U.S. Geol. Survey Prof. Paper 562*-g, 19 p.

Henderson, F.M., 1966. Open Channel Flow. MacMillan Pub. New York. 522 p.

Hicks, D.M., and Mason, P.D., 1991. Roughness characteristics of New Zealand Rivers: *Water Resources Survey DSIR Marine and Freshwater*, 329 p.

Hjulstrom, F., 1935. Studies of the morphological activity of rivers as illustrated by the River Fyris: *Bull. Geol. Inst. Univ. Upsala*, v. 25, pp. 221-528.

Hjulstrom, F., 1939. Transportation of detritus by moving water: *In Recent Marine Sediments*, P.D. Trask (editor)., pp. 51-70.

Holman, R.A., 1986. Extreme value statistics for wave run-up on a natural beach. *Coastal Engineering* v.9, pp. 527-544.

Hudson, R.Y., 1952. Wave forces on breakwaters. *Transactions of the American Society of Civil Engineers, ASCE,* v. 118, pp. 653-685.

Huges, M.G., 1995. Friction Factors for Wave Uprush.. *Journal of Coastal Research*, v. 11. 4, pp. 1089-1098..

Hunt, I.A., 1959. Design of seawalls and breakwaters. *Proc. ASCE*, 85: pp. 123-152.

Inman, D.L., 1949. Sorting of sediments in the light of fluid mechanics: *Jour. Sed. Petrology*, v. 19. pp. 51-70.

Iribarren, R., 1938. Una formula para el calculo de los disques de escollera. Revista de Obras Publicas, Madrid (A formula for the calculation of rock-fill dykes, translated by D. Heinrick, University of California, Dept. of Engineering *T.R.-He*-116-295 Berkeley, 1948.

Jarrett, R.D., 1984. Hydraulics of high-gradient Streams: *Jour. of Hydraulic Engineering,* A.S.C.E. 110(11), pp. 1513-1539.

Johnson, C.N., 1987. Rubble beaches versus revetments. *Proc. Coastal Sediments '87* American Society of Civil Engineers. v. 2, pp. 1217-1231.

Kellerhals. R., 1967. Stable channels with gravel-beds. Journ. of the Waterways and Harbors Division. ASCE, No. WW1, pp. 63-84.

Kirchner, J.W., Dietrich, W.E., Iseya, F., and Ikeda, H., 1990. The variability of critical shear stress, friction angle, and grain protrusion in water-worked sediments: *Sedimentology*, v. 37, pp. 647-672.

Kobayashi, N., Greenwald, J.H., 1986. Prediction of wave runup and riprap stability. *Coastal Engineering*, v. 10, pp. 1958-1971.

Kobayashi, N., Strzelecki, M.S., and Wurjanto, A., 1988. Swash oscillation and resulting sediment movement. *Coastal Engineering*, v. 12, pp. 1167-1181.

Kobayashi, N., and DeSilva, G., 1989. Wave transformation and swash oscillation on gentle and steep slopes. *Journal of Geo. Physical Res.* Vol. 94 C1: pp. 951-966.

Komar, P.D., 1976. *Beach Processes and Sedimentation*, Englewood Cliffs, N.J.:Prentice-Hall, 429 p.

Komar, P.D., and Gaughan, M.K., 1973. Airy wave theory and breaker height prediction. *Proc. 13th Conf. Coast. Eng.* v. 1, pp. 405-418.

Komar, P.D., and Zhenlin Li, 1986. Pivoting analyses of the selective entrainment of sediments by shape and size with application to gravel threshold: *Sedimentology*, v. 33, pp. 425-436.

Komar, P.D., 1987a. Selective gravel entrainment and the empirical evaluation of flow competence: *Sedimentology*, v. 34, pp. 1165-1176.

Komar, P.D. 1987b. Selective grain entrainment by a current from a bed of mixed sizes: A reanalysis: *Jour. Sed. Petrology* 57: No. 2, pp. 203-211.

Komar, P.D., 1988. Applications of grain-pivoting and sliding analyses to selective entrainment of gravel and to flow-competence evaluations: *Sedimentology*, v. 35, pp. 681-695.

Komar, P.D., 1989. Flow-competence evaluations of the hydraulic parameters of floods: an assessment of the technique. *In Floods: Hydrological, Sedimentological and Geomorphological Implications*, (K.Beven and P. Carling Editors) pp. 107-133.

Komar, P.D., and Carling, P.A., 1991. Grain sorting in gravel bed streams and the choice of particle sizes for flow-competence evaluations: *Sedimentology,* v. 38, pp. 489-502.

Komar, P.D., and Shih, S.M., 1992. Equal mobility versus changing grain sizes in gravel-bed streams. *In Gravel-bed Rivers:* Hey,R.D., Bathurst, J.C. and Thorne,C.R., pp. 73-106.

Lane, E.W. and Carlson, E.J., 1953. Some factors affecting the stability of canals constructed in coarse granular materials. *Proc. Int. Ass. Hydr. Res.* pp. 37-48.

Li, Zhenlin and Komar, P.D., 1986. Laboratory measurements of pivoting angles for applications to selective entrainment of gravel in a current: *Sedimentology,* v. 33, pp. 413-423.

Lisle, T. E., 1989. Sediment transport and resulting deposition in spawning gravels, North Coastal California. Water Resources Res. v. 25, No. 6 pp. 1303-1319.

Lorang, M.S., 1991. An artificial perched-gravel beach as a shore protection structure. *Proc. Coastal Sediments '91* American Society of Civil Engineers. v. 2, 1916-1925.

Milhous, R.T., 1973. Sediment transport in a gravel-bottom stream: Ph.D. thesis, Oregon State Univ., Corvallis, Oregon, 232 p.

Miller, M.C., McCave, I.N., and Komar, P.D., 1977. Threshold of sediment motion in unidirectional currents: *Sedimentology*, v. 24, pp. 507-528.

Nautical Software, 1996. Tides and Currents user guide. *Nuatical Software Inc.* Beaverton, Oregon.

Nicholls, R.J., 1988. Profile characteristics of shingle beaches. *Proc. 2nd European workshop on coastal zones,* Loutraki, Greece, Dept. of Civil Engr. National Technical University, Athens Greece.

Nicholls, R.J., 1990. Managing erosion problems on shingle beaches: Examples from Britain. *3rd European Workshop on Coastal Zones*, Paralimni,Cyprus. pp. 1-22.

Novak, I.D., 1969. Swash-zone competency of gravel sediment. *Marine Geology*, pp. 335-345.

Novak, P., and Nalluri, C. 1975. Sediment transport in smooth fixed bed channels. *Jour. of Hydraulics Div., Amer. Soc. Civil Engrs.*, v. 101, HY9, p. 1139-1154.

Novak, P., and Nalluri, C. 1984. Incipient motion of sediment particles over fixed beds. *Journ. Hydraulics Res.*, v. 22, pp. 181-197.

Oak, H.L., 1981. Boulder beaches: A sedimentological study. Ph.D. Thesis, Macquarie University, School of Earth Sciences, p.272.

Oak, H.L., 1985. Process inference from coastal-protection structures of boulder beaches. *Geogr. Ann.* 68, pp. 25-31.

O'Connor, J.E., 1993. Hydrology, Hydraulics and Geomorphology of the Bonneville Flood. *U.S. Geological Survey Special Paper* 274, Geological Society of America Pub. p. 83.

Orford, J.D., 1977. A proposed mechanism for storm beach sedimentation. *Earth Surface Processes*, v. 2, pp. 381-400.

Orford, J.D., Carter R.W.G. and Jennings, S.C., 1996. Control domains and morphological phases in gravel-dominated coastal barriers of Novia Scotia. *Journal of Coastal Res.* v. 12, pp. 589-604.

Parker, G., and Klingeman, P.C., 1982. On why gravel bed streams are paved: *Water Resources Res.*, v. 18, pp. 1409-1423.

Parker, G., Klingeman, P.C., and McLean, D.G., 1982. Bedload and size distribution in paved gravel-bed streams: *Jour. Hydraulics Div., Amer. Soc. Civil Engrs.*, v. 108, HY4, pp. 544-571.

Pilarczyk, K.W., and der Boer, K., 1983. Stability and profile development of coarse materials and their application in coastal engineering. *Report No. 293, Delft Hydraulics Laboratory.*

Powell, K.A., 1988. The dynamic response of shingle beaches to random waves. *Coastal Engineering*, 12: 1763-1773.

Reid, I., and Frostick, L.E., 1986. Dynamics of bedload transport in Turkey Brook, a coarse-grained alluvial channel: *Earth Surface Processes and Landforms*, v. 11, p. 143-155.

Ridder, J.R., 1967. Bed-material movement, Middle Fork Eel River, California. *Prof. Pap. U.S. Geol. Surv.* 575-C pp. 219-221

Scott, K.M. and Gravlee, C.G., 1968. Flood surge on the Rubicon R., California: hydrology, hydraulics and boulder transport. *Prof. Paper U.S. Geol. Surv.* 422-M, 38 p.

Shih, S.M., and Komar, P.D., 1990. Hydraulic controls of grain size distributions of bedload gravels in Oak Creek, Oregon, USA: *Sedimentology*, v. 37, pp. 367-376.

Shih, S.M., and Komar, P.D., 1990. Differential bedload transport rates in a gravel-bed stream: A grain-size distribution approach: *Earth Surface Processes and Landforms,* v. 15, pp. 539-552.

Shields, A., 1936. "Anwendung der Aehnlichkeitsmechanik und der Turbulenz-forscgung auf die Geschiebewegung" (Application of Similarity Principles and Turbulence Research to Bed-Load Movement), Mitteilungen der Preuss.Versuchsanst fur Wasserbau und Schiffbau, Berlin, no 26 (translation W.P. Ott and J.C. van Uchelen, S. C. S. Cooperative Laboratory, California Institute of Technology, Pasadena, Calif.

Shields, F.D., and Milhous, R.T., 1992. Sediment and aquatic habitat in river systems: *Jour. of Hydr. Engr.*, v. 118. pp. 669-687.

Shore Protection Manual (SPM)., 1984. 4th ed. 2 vols. U.S. Army Corps. of Engineers, Coastal Engineering Research Center, Waterways Experiment Station, Vicksburg, Miss. , Govt. Printing Office, Washington, D.C.

Silvester, R., and Hsu, J.R.C., 1993. Coastal Stabilization: Inovative Concepts. Prentice-Hall, New Jersey. 578 p.

Stanford, J.A., Ward, J.V., Liss, W.J., Williams, R.N., and Coutant, C.C., 1996. A general protocol for restoration of regulated rivers. *Regulated Rivers: Research and Management,* v. 12, pp. 391-413.

Sternberg, R.W., 1972. Predicting Initial Motion and Bedload Transport of Sediment Particles in the Shallow Marine Environmemt. *In: Shelf Sediment Transport*, D.J.P. Swift et al. editors. pp. 62-82.

Tillotson, K.J., 1994. Wave climate amd storm systems on the Pacific Northwest Coast: M.S.. thesis, Oregon State Univ., Corvallis, Oregon, 138 p.

Tillotson, K.J., and Komar P.D., 1997. The wave climate of the Pacific Northwest (Oregon and Washington): A comparison of Data Sources. Jour. of Coastal Res. v. 13., No. 2, pp. 440-452.

van der Meer J.W., and Pilarczyk, K.W., 1986. Dynamic stability of rock slopes and gavel beaches. *Proc. 20th Coastal Engineering,* American Society of Civil Engineers, 2, pp. 1713-1726.

van der Meer J.W., 1987. Stability of Breakwater Armour Layers-Design Formulae. *Coastal Engineering*, v. 11, pp. 219-239.

van der Meer J.W., 1988. Rock slopes and gravel beaches under wave attack. *Delft. Hydr. Communication* No. 396.

van der Meer J.W., 1992. Stability of the seaward slope of berm breakwaters. *Coastal Engineering,* v. 16, pp. 205-234.

van der Meer, J.W., and Stam, C.M., 1992. Wave run-up on smooth and Rock Slopes of Coastal Structures. *Jour. of Waterway Port, Coast, and Ocean Eng.* v. 118, pp. 534-550.

Vanoni, V.A., 1975. Sedimentation Engineering. *Amer. Soc. of Civil Engineers*, New York, N.Y.

Van Rijn, L.C. 1982. Equivalent roughness of an alluvial bed. *Journal of the Hydraulics division (ASCE)* HY10, pp. 1215-1218.

Von Guerard, P.B., 1989. Sediment transport characteristics and effects of sediment transport on benthic invertebrates in Fountain, Creek drainage basin upstream from Widefield, southeastern Colorado, 1985-1988: U.S. Geological Survey Water-Resources Investigations Report 89-4161, 133 p.

Voulgaris, G., Wilkin, M.P. and Collins, M., 1994. Shingle Movement Under Waves and Currents: An instrumented Platform for Field Data Collection. *Proc. Coastal Dynamics 94'* pp. 895-909.

Waal, J.P., and J.W. van der Meer., 1992. Wave Runup and Overtopping on Coastal Structures. *Coastal Engineering*, v16, pp. 1758-1771.

Wahl, K.L., 1993. Variation of Froude number with discharge for large-gradient streams. *Hydraulic Engineering* '93., v. 2 , pp. 1517-1522.

Wahl, K.L., and Miller, J.E., 1996. The occurence of critical and supercritical velocities in natural channels. *Stochastic Hydraulics '96,* Tickle, Goulter, Xu, Wasimi and Bouchart (eds) 1996 Balkema, Rotterdam. ISBN 90 54108177., pp. 561-568.

Ward, D.L., and Ahrens, J.P. 1991. Laboratory study of a dynamic berm revetment. *U.S. Army Corps of Engrs.* Coastal Eng. Res. Center, Waterways Experiment Station.

White, C.M., 1940. The equilibrium of grains on a bed of a stream. *Proc. Royal Soc. London Series A,* 174, pp.332-338.

Whiting, P.J., and Dietrich, W.E., 1990. *Boundary shear stress and roughness over mobile alluvial beds*: Jour. of Hydr. Engr., v. 116, No. 12, pp. 1495-1511.

Williams, G.P., 1978. *Bank-full discharge of Rivers. Water Resources Research.* v. 14., No. 6, pp.1141-1154.

Williams, G.P., 1983, Paleohydrological methods and some examples from Swedish fluvial environments. I. Cobble and boulder deposits: Geogr. Ann., 65A (3-4), pp. 227-243.

Wolman, M.G. and Eiler, J.P., 1958. Reconnaissance study of erosion and deposition produced by the flood of August 1955 in Connecticut. *Trans. Am. Geophys. Un.,* v. 39, pp. 1-14.

Yalin, M.S., and Karahan, E., 1979. Inception of sediment transport: *Jour. of the Hydraulics Division, Amer. Soc. Civil Engrs.* 105: (HY11), pp. 1433-1443.